Ingestion of Bacillus cereus spores dampens the immune response to favor bacterial persistence

Salma Hachfi, Alexandra Brun-Barale, Patrick Munro, Marie-Paule Nawrot-Esposito, Gregory Michel, Arnaud Fichant, Mathilde Bonis, Raymond Ruimy, Laurent Boyer, Armel Gallet

Ingestion of *Bacillus cereus* spores dampens the immune response to favor bacterial persistence

Salma Hachfi[1,2], Alexandra Brun-Barale[1], Patrick Munro[2], Marie-Paule Nawrot-Esposito[1], Gregory Michel[2], Arnaud Fichant[1,3], Mathilde Bonis[3], Raymond Ruimy[2,4], Laurent Boyer[2,✉] and Armel Gallet[1,✉]

[1]Université Côte d'Azur, CNRS, INRAE, ISA, France

[2]Université Côte d'Azur, Inserm, C3M, Nice, France

[3]Anses (Laboratoire de Sécurité des Aliments), Université Paris-Est, France

[4]Bacteriology Laboratory, Archet 2 Hospital, CHU, Université Côte d'Azur, Nice, France

✉Correspondence: **L. Boyer** (Laurent.BOYER@univ-cotedazur.fr), INSERM U1065, C3M, Bâtiment Universitaire ARCHIMED, 151 route Saint Antoine de Ginestière, BP 2 3194, 06204 NICE CEDEX 3 & **A. Gallet** (Armel.GALLET@univ-cotedazur.fr), ISA, 400 route des Chappes, BP 167, 06903 Sophia Antipolis Cedex, France

SUMMARY

Spores are considered as dormant entities highly resistant to extreme conditions. Among them, *Bacillus cereus* spores are commonly associated with foodborne outbreaks. Nevertheless, the pathological processes associated with spore ingestion and germination remain poorly understood. Here, we show that while ingestion of vegetative bacteria leads to their elimination from the midgut and small intestines of *Drosophila* and mice, respectively, a single ingestion of spores leads to the persistence of bacteria for at least 10 days. Using *Drosophila* genetics, we demonstrate that spores escape the innate immune response of the anterior midgut. Once in the posterior midgut, spores germinate, and the vegetative cells dampen the immune signaling through the induction of amidases which are negative regulators of the immune response. This study provides evidence for how *B. cereus* spores hijack the intestinal immune defenses allowing the localized birth of vegetative bacteria responsible for the digestive symptoms associated with foodborne illness outbreaks.

Keywords: Intestine; *Bacillus* spores; Innate immunity, Amidases, *Drosophila*, Mice

INTRODUCTION

Organisms are subjected to various environmental stresses including starvation, temperature variation, chemicals and microbes. Healthy individuals overcome these assaults by engaging defense mechanisms that maintain their homeostasis. Among the stressors, opportunistic enteric bacteria become pathogenic when host defenses are diminished or inefficient.

The evolutionarily conserved innate immune system is the first line of defense against bacteria, and adult *Drosophila* has proven to be a powerful model for innate immunity studies (Capo et al., 2019). In the midgut, the local innate immune system is mainly mounted in the anterior parts (Capo et al., 2019; Royet and Charroux, 2013). First, anterior enterocytes can rapidly sense the presence of allochthonous (i.e., non-commensal) bacteria and secrete reactive oxygen species (ROS) in a DUOX-dependent manner to block bacterial proliferation (Benguettat et al., 2018; Kim and Lee, 2014). Concomitantly, luminal ROS are perceived by a subpopulation of anterior enteroendocrine cells that respond by releasing the DH31/CGRP neuropeptide, which promotes visceral muscle spasms to provoke the expulsion of bacteria from the midgut in less than 4 hours post-ingestion (Benguettat et al., 2018). Nevertheless, if the load of allochthonous bacteria is higher and/or if the immune ROS and visceral spasms are insufficient to eliminate them, the allochthonous bacteria can start to proliferate, releasing muropeptides from the peptidoglycan (PGN), a bacterial cell wall component, that bind to the transmembrane and intracellular immune receptors PGRP-LC and PGRP-LE, respectively (Bosco-Drayon et al., 2012; Kaneko et al., 2006). Consequently, the Immune deficiency (Imd)/NF-κB pathway is activated, leading to the expression of anti-microbial peptides (AMPs) beginning 4-6 hours post-ingestion (Bonfini et al., 2016; Buchon et al., 2009b; Chakrabarti et al., 2012; Zhai et al., 2018b). Because a prolonged activation of the local innate immunity is responsible for chronical inflammation which is detrimental for the individual, a robust negative feedback is turned on to tune down the Imd pathway once the bacteria are

cleared (Zhai et al., 2018b). For instance, the PGRP-SC1 & 2 and PGRP-LB amidases have been described as negative regulators of the Imd pathway mainly acting by digesting the extracellular PGN fragments and thus blocking the recognition process by the Imd pathway receptors (Costechareyre et al., 2016; Guo et al., 2014; Kaneko et al., 2006; Paredes et al., 2011). Altogether, these combined means of defense allow an efficient sensing and elimination of the allochthonous bacteria allowing the survival of the individual.

However, the detection of bacterial spores by the local innate immune system of the intestine and their elimination remains challenging for host organisms. Indeed, spores can resist many biological, chemical, or physical treatments (Ehling-Schulz et al., 2019; Setlow, 2014). Among opportunistic bacteria, the widespread environmental spore-forming bacteria belonging to the *Bacillus cereus* (*Bc*) group are well-known worldwide food poisoning pathogens that cause diarrheal and/or emetic-type illnesses (Dietrich et al., 2021; Jovanovic et al., 2021). *Bc* is the second most important cause of foodborne outbreaks (FBOs) in France (Bonis et al., 2021; Glasset et al., 2016; Santé publique France, 2019) and the third in Europe (EFSA and ECDC, 2018). When nutrient-rich conditions are encountered, *Bc* spores can germinate, giving rise to vegetative cells which can even proliferate. Such favorable conditions are present in the small intestine of mammals, where it is assumed that spores are able to germinate and probably proliferate to ultimately trigger diarrhea due to the production of enterotoxins (Berthold-Pluta et al., 2015; Ehling-Schulz et al., 2019). *In vitro* experiments have indicated that *Bc* vegetative cells can be destroyed by the acidic pH of the stomach and the biliary salt of the duodenum while spores can resist (Barbosa et al., 2005; Berthold-Pluta et al., 2015; Ceuppens et al., 2012a; Ceuppens et al., 2012b; Ceuppens et al., 2012c; Clavel et al., 2004). The effectiveness of the gut innate immune system to fight *Bc* vegetative cells has been demonstrated (Benguettat et al., 2018). In contrast, nothing is known concerning the

behavior and the fate of *Bc* spores in the intestine *in vivo* and the related immune response mounted by the host.

Here, thanks to *in vivo* studies, we demonstrate that spores germinate only in the posterior parts of the *Drosophila* midgut and of the mouse small intestine. We show that bacteria of *Bc* group can persist for at least ten days in the posterior regions of the midgut/small intestine. Next, we demonstrate that the spores do not trigger any detectable immune responses in the anterior parts of the *Drosophila* midgut. Once in the posterior midgut, germinated cells trigger the Imd immune pathway in a PGRP-LE dependent manner. Strikingly, we found the amidases PGRP-SC1/2 and PGRP-LB, which are negative regulators of the Imd pathways, to be induced while the AMPs were repressed. In flies deficient in the PGRP-LE receptor, the cytosolic members of the Imd pathway or the PGRP-SC1/2 and PGRP-LB amidases, the persistence of the bacteria in midgut was reduced. Surprisingly, removing Relish, the NF-κB-like transcription factor, downstream of the Imd pathway has no impact on the bacterial persistence. However, depletion of Dif, another NF-κB-like transcription factor, together with Relish provided the proof of a critical cooperation of both transcription factors in regulating *amidase* and *AMP* expressions in the posterior midgut and thus the bacterial clearance. Altogether, we provide evidence that spores belonging to the *Bc* group persist in the intestine when ingested as spores and escape the anterior immune response. Spores reach the posterior regions of the midgut where they germinate, and vegetative bacteria induce expression of amidases that act as negative regulators of the Imd pathway, dampening the production of AMPs, consequently fostering the persistence of the bacteria.

RESULTS

Spores of the *Bc* group persist in the *Drosophila* intestine

The *Bc* group is subdivided into at least eight phylogenetically very close genomospecies (Carroll et al., 2021; Carroll et al., 2020; Ehling-Schulz et al., 2019). For this study, we selected the reference strain *Bc sensu stricto (Bc* ATCC 14579) as well as two *Bacillus thuringiensis* subspecies *kurstaki* (*Btk*) strains (*Btk* SA-11 and *Btk* ABTS-351) because of their broad use as microbial pesticides and the fact that *Btk* has been suspected to be responsible for FBOs (Biggel et al., 2021; Bonis et al., 2021; Johler et al., 2018).

To determine whether, upon ingestion, *Bc* or *Btk* spores behaved the same as vegetative cells, we fed flies continuously with contaminated food and assessed the amount of *Bc* or *Btk* bacteria in the *Drosophila* midgut at different times (Figure 1A). We observed that regardless of the strain used, *Bc*/*Btk* were still present in the *Drosophila* midgut at least 10 days after the initial contact with spore-contaminated food (Figure 1B).

These data were very different from what we observed using *Bc* ATCC 14579 or *Btk* SA-11 vegetative cells, whose loads in the intestine rapidly decreased within 24 hours (Figure S1A). Unlike *Bc*, during sporulation, *Btk* produces Cry toxins embedded in a crystal, which displays specific entomopathogenic properties. *Btk* is widely used specifically to kill lepidopteran larvae that are broad crop pests (Ehling-Schulz et al., 2019). Because the presence of Cry toxins might influence the behavior of *Btk* in the midgut, we engineered a *Btk* SA-11$^{\Delta Cry}$ strain cured of its plasmids and therefore devoid of Cry toxins (see Experimental Procedures). We also used a *Btk*$^{\Delta Cry}$ obtained from the Bacillus Genetic Stock Center (#4D22, https://bgsc.org/) also devoid of Cry toxins. Importantly, the SA-11$^{\Delta Cry}$ and the *Btk*$^{\Delta Cry}$ spores behaved like *Btk* SA-11 and *Bc* ATCC 14579 spores (Figure 1B), refuting any possible role of the Cry toxins in this phenomenon. The commercially available preparation of the *Btk* ABTS-351 spores is known to contain 46% of additives (ec.europa.eu). To assess the potential involvement of those additives in the intestinal persistence of *Btk* ABTS-351, we extended our study to the commercial preparation, which we compared with a *Btk* ABTS-351 spore

preparation made in our laboratory without any additives. We noticed that the commercial spores as well as the "homemade" *Btk* ABTS-351 spores behave similarly in the *Drosophila* midgut (Figure 1B and S1B), suggesting that the additives present in the commercial preparation did not contribute to the persistence of *Btk* ABTS-351 spores.

Because spores could germinate and proliferate on the fly medium, we checked this possibility by counting the number of *Btk* SA-11 bacteria on the fly medium in the absence of flies. We applied a heat treatment in order to kill all germinated vegetative cells. We noticed that 2 days after spore deposit on the fly medium, some of them started their germination and even proliferated 4 days after deposit (Figure S1C). Hence, to remove this limitation in the persistence assessment, we performed acute feeding. Flies were fed with spores for 30 min before being transferred onto fresh food medium (i.e. without spores) (Figure 1C). We first verified that upon acute ingestion of *Bc* ATCC 14579 or *Btk* SA-11 vegetative cells, they were readily cleared from *Drosophila* midguts (Benguettat et al., 2018) (Figure S1D). We then monitored the persistence of spores in the *Drosophila* midgut upon acute feeding (Figure 1D). After 30 min of spore feeding, the bacterial load averaged 10^4 cells per midgut regardless of *Bc*/*Btk* strain. Interestingly, the bacteria could persist up to 10 days in the *Drosophila* midgut after acute spore ingestion (Figure 1D and S1E). The same observation was made with *Btk* SA-11 spores in a different *Drosophila* genetic background (i.e., w^{1118} *Drosophila* midgut, Figure S1F). These results demonstrate that, unlike ingestion of vegetative cells, ingestion of *Bc*/*Btk* spores results in bacterial persistence for several days in the *Drosophila* midgut.

The *Drosophila* midgut is subdivided into five major anatomical regions (R1 to R5) (Figure S1G) (Buchon et al., 2013; Marianes and Spradling, 2013). To analyze in detail the localization of *Bc*/*Btk* along the midgut, we quantified the bacterial load in the anterior and posterior midgut after acute feeding. We did not focus on the acidic region due to its small size and the difficulty to dissect it accurately. During the first two hours after acute ingestion,

we found that *Bc*/*Btk* bacteria were present in both regions of the midgut (anterior and posterior). However, from 4 hours onward, the posterior midgut harbored a significantly higher load of *Bc*/*Btk* cells compared with the anterior midgut (Figure 1E). Collectively, our results demonstrate that *Bc*/*Btk* persist for up to 10 days in the midgut and may accumulate preferentially in the posterior regions.

Spores of the *Bc* group germinate preferentially in the posterior midgut

Spores are metabolically dormant and resistant to extreme environmental conditions, allowing them to survive to extreme conditions (Setlow, 2014). However, the presence of nutrients can trigger the process of germination, in which spores emerge from dormancy, growing into vegetative cells. Since the intestine is a favorable environment for spore germination, we hypothesized that *Bc*/*Btk* spores might germinate in the *Drosophila* midgut. To address this question, we developed a robust fluorescent staining technique suitable for visualizing spores and differentiating them from their outgrowing vegetative cells. Dormant *Bc*/*Btk* spores harbored a red fluorescence. Once germinated, vegetative cells started to express the green fluorescent protein (GFP). The use of this novel tool endowed with dual red/green (R/G) labelling allowed us to follow the process of germination in real time (Figure 2A, movie1).

The use of the *Btk* SA-11$^{R/G}$ fluorescent strain *in vivo* first revealed that at 0.5- and 2-hours post-ingestion, *Btk* spores occupied the lumen of the whole midgut (Figure S2A and S2B). Few vegetative cells were detectable in the posterior midgut 2 hours post-ingestion (inset in Figure S2B). *Btk* SA-11$^{R/G}$ spore germination was evident in the posterior midgut 4 hours after ingestion (Figures 2B and 2C). Interestingly, we found that regardless of the *Bc* group strain, spore germination occurred markedly in the *Drosophila* posterior midgut at 4 hours after ingestion (Figure S2D). Twenty-four hours post-ingestion, we detected mostly vegetative cells in the posterior midgut (Figure S2C). To further confirm that spores mainly germinated in the posterior midgut, we performed measurements of colony-forming units

(CFUs) in the anterior and posterior parts of the midgut by comparing heat-treated intestinal samples (to kill germinating spores and vegetative cells but not spores) to non-heat-treated samples (cumulating spores, germinating spores and vegetative cells). Interestingly, we did observe in the anterior midgut region the almost exclusive presence of *Bc*/*Btk* spores, even 3 days after acute ingestion (Figure 2D). However, in the posterior midgut, we observed the appearance of the first *Bc*/*Btk* germinating spores as early as 30 minutes after ingestion (Figure 2E). Together, these results demonstrate that the germination of *Bc* group spores begins 30 minutes after oral ingestion and occurs mainly in the posterior midgut of *Drosophila melanogaster*.

Spores do not trigger detectable *Drosophila* midgut innate immune response

The persistence of spores in the *Drosophila* midgut raises the question of how the local innate immune system can tolerate spores and/or vegetative cells. As mentioned previously, in response to enteric infection, the anterior *Drosophila* midgut (R1 and R2 regions) initiates immune responses via the luminal release of ROS and, if necessary, AMPs (Benguettat et al., 2018; Bosco-Drayon et al., 2012; Hachfi et al., 2019; Lee et al., 2013; Royet and Charroux, 2013; Tzou et al., 2000). To test the release of local immune ROS (HOCl) in response to *Btk* vegetative cells or spores, we used the R19S probe, a HOCl sensitive fluorescent dye (Chen et al., 2011; Hachfi et al., 2019). First, we confirmed that *Btk* vegetative cells induced ROS only in the anterior region one-hour post-ingestion (Figure 3A, middle panel). Surprisingly, *Drosophila* fed with *Btk* spores did not show ROS induction either in the anterior or in the posterior regions of the *Drosophila* midgut (Figure 3A, lower panel), though spores germinated in the posterior midgut (Figures 2 and S2). In parallel, we specifically knocked down the expression of *Duox* in *Drosophila* enterocytes by RNA interference and examined the resulting impact on the spore persistence. We first confirmed that, 4 hours after ingestion of vegetative cells, the silencing of *Duox* in the enterocytes increased the load of *Btk*

compared with control intestines (Benguettat et al., 2018) (Figure 3B). However, *Duox* silencing in *Drosophila* enterocytes did not impact the *Btk* persistence after spore ingestion (Figure 3B). Based on these data, we inferred that ingestion of spores does not induce the production of *Duox*-dependent ROS.

We next investigated the induction of *AMP* genes in the *Drosophila* midgut following acute ingestion of vegetative cells vs. spores. Using the *DiptericinA-Cherry* (*DptA-Cherry*) and *AttacinD-Gal4 UAS-Cherry* (*AttD>Cherry*) reporters, two readouts for the activation of the Imd pathway in the midgut (Charroux et al., 2018), we first observed that the acute ingestion of vegetative cells of the *Erwinia carotovora carotovora* (*Ecc15*) opportunistic bacteria induced *DptA* and *AttD* expression in the anterior midgut (Figure 3C, 3D, S3A and S3B). *Ecc15* was also capable of promoting the spreading of *AttD* expression in the posterior R4 region (Figure S3B). However, *Btk* vegetative cells did not show significant changes in *DptA* expression in either the anterior or posterior midgut (Figure 3C and S3A), while *AttD* was slightly induced, though not significantly, in the anterior midgut (Figure 3D). These data are consistent with the fact that early ROS induction followed by the visceral spasms are sufficient to rapidly eliminate *Btk* vegetative cells upon acute ingestion (Figure 3A and 3B) (Benguettat et al., 2018), at least before the Imd pathway can be induced. RT-qPCR analyses of the expression of *DptA, Defensin and AttD* genes on dissected midguts confirmed the non-induction of *AMP* genes after acute ingestion of *Btk* (or *Bc*) vegetative cells (Figure S3C).

Monitoring *AMP* expression upon acute spore feeding revealed that neither *DptA-Cherry* nor *AttD-Cherry* reporter genes were induced *in vivo* in the anterior midgut (Figure 3C, 3D, S3A and S3B). Strikingly, repression of the *DptA-Cherry* reporter expression in the posterior midgut was observed (Figure 3C and S3A). RT-qPCR analyses confirmed the repression of *DptA* expression as well as the repression of *Defensin* and *AttD* expression

(Figure 3E). Together these data suggest that *Bc/Btk* persistence upon spore ingestion could be supported by decreased expression of *AMPs*.

To assess the involvement of the AMPs in *Btk* SA-11 persistence, we used a fly strain in which the 14 *AMP* genes were deleted (ΔAMP^{14}) (Carboni et al., 2021; Hanson et al., 2019). We quantified the *Btk* SA-11 load in the midgut of wild type (*Canton S*) and ΔAMP^{14} flies. While both genotypes ingested a similar amount of spores during the 30 min of feeding (Figure 3F), 120h post-feeding, in ΔAMP^{14} mutant flies, we found a significantly higher *Btk* SA-11 load compared with wild-type flies (Figure 3F). This result suggests that AMPs could kill germinating cells in the posterior midgut. To further challenge this hypothesis, we monitored the fate of the *Btk* SA-$11^{R/G}$ fluorescent strain in ΔAMP^{14} mutant flies after acute ingestion of spores. As expected, two hours post-ingestion, confocal imaging showed higher levels of germinating spores in ΔAMP^{14} mutant posterior midguts than in WT posterior midguts (Figure 3G). We did not observe obvious changes in the anterior midguts where only spores were present (Figure 3G). Collectively, our data suggest that, though repressed upon spore ingestion, the weak production of AMPs is necessary to limit the *Bc/Btk* bacterial load in the posterior midgut.

Amidases contribute to the intestinal persistence of spores

Since *AMPs* expression was downregulated after spore ingestion, we wondered whether the amidases, which exert negative feedback on the Imd pathway, could be induced by germinating spores (Charroux et al., 2018; Costechareyre et al., 2016; Paredes et al., 2011). First, we verified by RT-qPCR analyses that the ingestion of *Bc/Btk* vegetative cells could induce the expression of the three *amidase* encoding genes in the midgut (Figure S4). Interestingly, after spore ingestion, we observed that PGRP-SC1 and -SC2 were consistently induced both 4 hours and 24 hours post-feeding while PGRP-LB was only induced at 4 hours and was repressed at 24h hours (Figure 4A). We next assessed the *Btk* SA-11 intestinal load in

mutant flies homozygous for either the *PGRP-SC1/2* or *PGRP-LB* loss-of-function alleles (*PGRP-SC1/2*$^{\Delta}$ and *PGRP-LB*$^{\Delta}$ respectively) (Paredes et al., 2011). In midguts from these mutant animals, no difference in bacterial load was observed compared with control flies 30 min after spore feeding (Figure 4B). However, 120 hours post-feeding, the loss of *PGRP-SC1/2* or *PGRP-LB* was associated with a significant decrease in the number of *Btk* SA-11 in the midgut compared with the *Canton S* flies (Figure 4B). Because spores accumulated and germinated in the posterior midgut of *Canton S* flies as early as 4 hours post-ingestion (Figure 2), we monitored the fate of the spores in *PGRP-SC1/2*$^{\Delta}$ and *PGRP-LB*$^{\Delta}$ deficient flies. Six hours after acute ingestion, confocal imaging showed the presence of fewer red/green germinating spores in the posterior midguts of *PGRP-SC1/2*$^{\Delta}$ or *PGRP-LB*$^{\Delta}$ flies compared with WT flies (Figure 4C), suggesting that in the absence of amidases, the production of AMPs was able to kill germinating spores.

We therefore investigated whether the repression of *AMPs* expression upon spore ingestion was indeed dependent of amidases. As expected, expression of *AMPs* was not repressed; indeed, it was even induced by *Btk* SA-11 spore ingestion in a *PGRP-SC1/2*$^{\Delta}$ or *PGRP-LB*$^{\Delta}$ mutant background (Figure 4D compared with 3E). Because Amidases can be produced by the enterocytes or by the fat body (a systemic immune tissue) and can act at a distance from the site of production (Charroux et al., 2018), we specifically silenced *PGRP-SC2* or *PGRP-LB* in enterocytes and found a significant decrease in the load of *Btk* SA-11 in the midgut (Figure 4E). Overall, our data suggest that spores are not detected by the anterior midgut immune response (i.e., no production of ROS or AMPs), and reach the posterior regions where they germinate and can activate the Imd signaling target genes *PGRP-SC1*, *PGRP-SC2*, and *PGRP-LB*. In turn, Amidases promote a repression of basal expression of AMP-encoding genes. Consequently, downregulation of *AMP* expression favors *Bc/Btk* persistence in the posterior *Drosophila* midgut.

The Imd pathway contributes to the spore intestinal persistence

Because the expression of *amidases* is under the control of the Imd pathway in the intestine, we first tested the involvement of the two Imd pathway receptors, PGRP-LC and -LE, in *Btk* SA-11 persistence. In flies homozygous viable for the loss-of-function mutant for either receptor, similar amounts of *Btk* SA-11 were ingested compared with WT flies after 30 minutes of spore feeding (Figure 5A). Nevertheless, 120 hours after feeding, only *PGRP-LE*^{112} mutant flies showed a significant decrease in *Btk* SA-11 intestinal load (Figure 5A) similar to that observed for flies lacking the amidases (Figure 4B). These results show that PGRP-LE contributes to the sensing of germinated spores in the posterior midgut and confirm that PGRP-LE is the primary receptor in the posterior midgut that regulates amidase expression (Bosco-Drayon et al., 2012).

We further tested mutants for intracellular components of the Imd pathway. Loss-of-function mutants for the cytoplasmic components Imd (*imd*^{Shaddok}) or Dredd (*Dredd*^{F64}) also displayed a decrease in *Btk* SA-11 persistence 120 hours post-ingestion (Figure 5B). Unexpectedly, the bacterial load in flies homozygous mutant for the downstream Imd pathway NF-κB-like transcription factor Relish (*Rel*^{E20}) (Hedengren et al., 1999) was similar to control flies (Figure 5C), although Rel has been found to be absolutely required in midgut epithelial cells to respond to enteropathogenic bacteria (Bosco-Drayon et al., 2012; Buchon et al., 2009b; Vodovar et al., 2005). To confirm the absence of *Rel* function in our model of spore infection, we inhibited *Relish* expression specifically in enterocytes. Silencing *Relish* in enterocytes did not change *Btk* bacterial abundance in the midgut (Figure 5D). In addition, we monitored the fate of the *Btk* SA-11$^{R/G}$ fluorescent strain in *Rel*^{E20} mutants, six hours after acute ingestion. No obvious differences between *CantonS* and *Rel*^{E20} were observed in the *Drosophila* midgut (Figure 5E), confirming that the transcription factor Relish had no

significant role in the control of the germination and the persistence of *Btk* in the posterior midgut.

Given these observations, we wanted to test the involvement of Rel in controlling the remaining *AMP* expression in WT flies fed with spores (Figure 3E). We therefore performed qRT-PCR to measure the expression of the same *AMPs* in Rel^{E20} mutant flies, either fed, or not, with spores. While *DptA* and *Defensin* were drastically downregulated in the absence of Rel at 4 hours (Figure 5F) and 24 hours (Figure S5A) in unchallenged flies or after spore ingestion, *AttD* expression was not affected in Rel^{E20} flies, regardless of whether they were fed with spores (Figures 5F and S5A). In addition, the absence of Rel correlated with the downregulation of *PGRP-SC1a/b* and *PGRP-LB* expression (Figures 5G and S5B compared with 4A) but, unexpectedly, *PGRP-SC2* was strongly induced, even in the absence of spore ingestion (Figures 5G and S5B). The above data suggest that the expression of *PGRP-SC2* and, to a lesser extent, *AttD* in the posterior midgut are independent of the transcription factor Rel.

Taken together our data demonstrate that the Imd pathway can sense *Bc*/*Btk* geminating cells in the posterior midgut in a PGRP-LE-dependent manner in order to activate the expression of the amidases. In turn, amidases provoke a reduction of AMPs expression by tuning down the Imd pathway. Consequently, the decrease in AMP levels favor the local *Bc*/*Btk* persistence in the posterior midgut. Nevertheless, the most downstream component of the Imd pathway, Rel, appears not to be required.

Dif cooperates with Relish to modulate the intestinal immune response to spore ingestion

These data prompted us to investigate the possible involvement of another NF-κB-related transcription factor in the *Drosophila* posterior midgut, the Dorsal-related immunity factor (Dif), known to act downstream of the Toll pathway during the systemic immune response (Manfruelli et al., 1999; Meng et al., 1999; Petersen et al., 1995; Rosetto et al., 1995). To

understand whether Dif could also be involved in *Bc/Btk* persistence, we took advantage of flies homozygous viable for the *Dif* loss-of-function allele, Dif^{1}. While Dif^{1} and WT flies ingested similar amounts of spores during the 30 minutes of feeding, 120 hours later, we observed a significant decrease of *Btk* SA-11 loads in Dif^{1} mutant flies (Figure 6A). Confocal microscopy analysis confirmed the decrease of *Btk* SA-$11^{R/G}$ fluorescent cells, primarily in the posterior midguts of Dif^{1} mutant flies, compared with WT (Figure 6B). To further analyze the role of Dif in the intestinal immune response, we monitored the expression of *AMPs* and *amidases* in Dif^{1} mutant flies by qRT-PCR. In uninfected flies, the expression of *DptA* and *Defensin* was significantly lowered in the mutant compared with WT, while *AttD* was only slightly affected (Figures 6C and S6A). Feeding Dif^{1} mutant flies with spores did not promote any induction or repression of *AMPs* (Figures 6C and S6A). Regarding the expression of *amidase*s, while they were all induced in a WT background upon spore ingestion (Figure 4A), in the absence of Dif, the expression of *PGRP-SC1* level was lower, while *PGRP-LB* remained inducible by the ingestion of spores (Figures 6D and S6B). Notably, contrary to what we observed in Rel^{E20} mutants, *PGRP-SC2* was not upregulated in the absence of Dif (compare Figures 6D and S6B with Figures 5G and S5B).

To confirm the cooperation of both NF-κB factors in regulating the expression of *amidases* and *AMPs* in the posterior midgut, we generated a Dif^{1}*;* Rel^{E20} double mutant flies. We first monitored *Btk* persistence upon spore ingestion in this genetic background. Dif^{1}*;* Rel^{E20} double mutant and WT flies ingested a similar amount of spores during the 30 minutes of feeding (Figure 6E). However, 120 hours later there was a significantly higher *Btk* SA-11 load in the double mutant flies compared with WT (Figure 6E). Consistently, 6 hours after ingestion of *Btk* SA-$11^{R/G}$ spores, more fluorescent bacteria were present in the posterior midguts of Dif^{1}*;* Rel^{E20} double mutant flies compared with WT (Figure 6F). In this double

mutant background, the expressions of *AMPs* and *amidases* were lowered (Figures 6G, 6H, S6C and S6D).

Together our data suggest that Dif and Relish cooperate to regulate the expression of *DptA*, *Defensin* and *PGRP-SC1*, while Dif and Rel likely act redundantly to regulate the expression of *AttD*. Moreover, Relish and Dif have opposite effects on *PGRPSC-2* expression: Relish represses *PGRPSC-2* while Dif activates it. Finally, *PGRP-LB* expression appears to be regulated only by Relish. Overall, these results demonstrate that Dif and Relish cooperate to tightly balance the expression of AMPs and amidases in the posterior midgut of unchallenged as well spore-fed flies.

Bacillus spore persistence leads to _amidase_ expressions in the mouse gut

Because the *Bc* group is involved in human digestive illnesses, we wondered whether their spores could also persist in the intestine of mammals. We, therefore, investigated the fate and behavior of spores in the mice. In *Drosophila* midguts, all the spores we have studied behave similarly (Figures 1, S1, 2 and S2), therefore, to ethical considerations in mouse experiments, we restricted our experiments to the *Btk* SA-11 strain. Mice were fed with vegetative cells or spores using oral gavage (Figure 7A). In mammals, the small intestine is divided into three functional sections: the duodenum, the jejunum, and the ileum. Despite the duodenum being smaller than the other two more posterior regions of the small intestine, we decided to split the small intestine into three equivalent domains since there is no obvious anatomical distinction (Figure S7A).

As expected, we first found that upon gavage with vegetative cells, *Btk* SA-11 were rapidly cleared from the small intestines of mice (Figures S7B and S7C) within a time frame similar to that of *Drosophila*. By contrast, gavage with spores led to the detection of *Btk* SA-11 in the small intestine (equivalent to the *Drosophila* midgut) 240 hours post-oral-gavage (Figure 7B) as in *Drosophila* midguts. To monitor the spore germination, we performed CFU

379 measurements in heat-treated *vs* non-heat-treated intestinal samples. We found that 4 hours
380 post-gavage, *Btk* SA-11 spores were evenly distributed all along the small intestine and that
381 vegetative cells were more abundant in the ileum (Figure 7C). The few vegetative cells we
382 detected in the duodenum could be explained by the 1/3 splitting method we used that
383 encompassed the whole duodenum and likely part of the anterior jejunum (Figure S7A). We
384 also observed an obvious *Btk* SA-11 germination localized in the jejunum and ileum, 24 hours
385 onwards post-gavage (Figure 7C). Next, to confirm the timing and locations of spore
386 germination in the mouse intestine, we forced-fed our mice with the *Btk* SA-11$^{R/G}$ strain. Two
387 hours post-gavage, *Btk* SA-11$^{R/G}$ spores were localized throughout the small intestine and few
388 vegetative cells were detectable in the posterior ileum (Figure S7D). Four hours post-gavage,
389 *Btk* SA-11$^{R/G}$ vegetative cells occupied the posterior part of the jejunum and the ileum (Figure
390 7D). Twenty-four hours post-gavage, we detected mostly vegetative cells throughout the
391 jejunum and the anterior part of the ileum (Figure S7E). Notably, spores were evenly
392 distributed along the small intestine at the different time points analyzed (Figures 7D and S7D
393 and S7E). Together, these results suggested that spores persist and germinate in the
394 mammalian posterior small intestine regions, similar to our observations in the *Drosophila*
395 midgut.

396 However, as rodents are known for coprophagy, the data obtained above might be due
397 to continuous ingestion of spores beyond initial gavage (Kenagy and Hoyt, 1979). Consistent
398 with this, we detected *Btk* SA-11 spores in fecal samples up to ten days post-gavage (Figure
399 S7F). To prevent this, we frequently changed breeding cages (Figure 7E). As shown in
400 (Figure 7F), *Btk* SA-11 bacteria were detectable 24 hours post-gavage in the small intestine of
401 all mice (n=10). Interestingly, two mice still harbored *Btk* SA-11 bacteria 240 hours post-oral-
402 gavage by spores. We then monitored spore germination using CFU measurements in heat-
403 treated *vs* non-heat-treated intestinal samples. Four hours post-gavage, *Btk* SA-11 spores were

404 evenly distributed all along the small intestine, and vegetative cells were more abundant in the
405 ileum (Figure 7G). Twenty-four hours post gavage, we also observed *Btk* SA-11 germination
406 preferentially localized in the jejunum and ileum (Figure 7G). Later, *Btk* SA-11 spores were
407 still detectable in the duodenum, while vegetative cells were barely detectable. Ten days after
408 gavage, only vegetative cells were detected in the jejunum and ileum (Figure 7G).
409 Collectively, our results demonstrate that spores can persist for several days in the mouse
410 small intestine and germinate preferentially in the posterior part of the small intestine, the
411 jejunum and the ileum, similar to our observations in *Drosophila* midguts.

412 Finally, we explored the possibility that the two mouse orthologs of the *Drosophila*
413 amidases Pglyrp-1 and Pglyrp-2 (Lee et al., 2012; Osanai et al., 2011), might be upregulated
414 in response to spore ingestion. The expression of *Pglyrp-1* and *Pglyrp-2* genes was monitored
415 in the murine small intestine by quantitative RT-qPCR upon gavage with *Btk* SA-11 spores,
416 with or without changing the breeding cages (Figures 7A and 7E). We observed, 4- and 24-
417 hours post-gavage, an upregulation of *Pglyrp-1* only in the jejunum (Figure 7H and 7I),
418 whereas *Pglyrp-2* was upregulated both in the jejunum and ileum without changing the
419 breeding cage (Figure 7H) and only in the jejunum upon frequent breeding cage change e to
420 avoid continuous consumption (Figure 7I). These results demonstrate that spores can persist
421 in the small intestine of mice, germinate in the posterior parts, and trigger the expression of
422 amidases. Altogether our data suggest an evolutionarily conserved role for amidases in the
423 innate immune response and in tolerance to bacterial spores.
424

425 ## DISCUSSION

426 The majority of *Bc*-dependent FBOs, is due to the ingestion of *Bc* bacteria, which must grow
427 in the gut and subsequently produce pore-forming enterotoxins responsible for the onset of
428 diarrhea symptoms (Jovanovic et al., 2021). However, the mechanisms by which *Bc* bacteria

colonize the gut and produce toxins remain poorly understood, and several questions unanswered. Is the disease due to the ingestion of vegetative bacteria or spores? What is the distribution and the fate of ingested spores along the gastrointestinal tract? How does the intestinal innate immune system detect and fight the infection? Here, we deciphered the behavior and fate of *Bc* cells in the intestine of both *Drosophila melanogaster* and mouse, and demonstrated that spores escape the innate immune system to reach the posterior part of the midgut/small intestine, where they can germinate and persist for days within the animal.

First of all, our findings confirm *in vivo* that after ingestion of vegetative cells, the *Bc* load in the *Drosophila* and mouse intestine remains low and that the bacteria are cleared in less than 24 hours (Benguettat et al., 2018; Loudhaief et al., 2017; Rolny et al., 2014). In *Drosophila*, it has also been shown that the presence of vegetative cells in the anterior midgut is rapidly detected, triggering the production of ROS and visceral spasms, both cooperating to quickly evict the undesired bacteria (Benguettat et al., 2018). Therefore, the minimum infectious dose required to cause intestinal disorders (at least 10^5 CFU, (Berthold-Pluta et al., 2015)) is likely difficult to reach upon ingestion of vegetative cells. On the contrary, it has been suggested that the capacity of spores to withstand extreme conditions would allow them to overcome stomach acidity and bile salt attacks in the duodenum, favoring germination in the posterior small intestine. Consequently, the infectious dose could be more readily achievable, as illustrated by the 10^3 spores/g of food that can be associated with FBOs (Bonis et al., 2021; EFSA BIOHAZ, 2016). Importantly, our *in vivo* data reveal the conserved fate and behavior of spores in the intestine of *Drosophila* and mice. The spores of all *Bc* group strains we tested persisted up to 10 days post-ingestion. Consistent with our observations, studies have shown that *Bc* can persist at least 18 days in the intestine of rats transplanted with human-flora (Wilcks et al., 2008) and 30 days in mouse intestine (Oliveira-Filho et al., 2009). Moreover *Bt* could be detected in fecal samples in greenhouse workers five days after

454 cessation of bioinsecticide use (Jensen et al., 2002). Interestingly, we also showed *in vivo* that
455 spores accumulate and germinate in the posterior part of the *Drosophila* midgut and mouse
456 small intestine. Similarly, data suggest that spores derived from the probiotic *B. subtilis*
457 germinate in the jejunum and eventually in the ileum of mice (Casula and Cutting, 2002; Tam
458 et al., 2006). Our data also highlight the very rapid germination of spores in the posterior parts
459 of the intestine (in less than 2 hours). Indeed, while the proximal regions of the *Drosophila*
460 midgut and mouse small intestine are quite acidic and produce digestive enzymes to break
461 down food, the more distal parts of the intestine harbor a more basic and anaerobic
462 environment with nutrient availability (Marianes and Spradling, 2013; Osman et al., 2012;
463 Shanbhag and Tripathi, 2009). Interestingly, it has been shown, *in vitro*, that anaerobic
464 conditions slow down the growth rate of *Bc* but favor the production of CytK, Nhe and Hbl
465 enterotoxins (Berthold-Pluta et al., 2015; Duport et al., 2004; Duport et al., 2006; Jovanovic et
466 al., 2021; Miller et al., 2021; van der Voort and Abee, 2009; Zigha et al., 2006). Hence, all the
467 conditions for spore germination and enterotoxin production are encountered in the posterior
468 *Drosophila* midgut and mouse small intestine, which accounts for the occurrence of diarrheic
469 symptoms when a critical bacterial load is reached.

470 Importantly, our data also show that the local innate immune response is ineffective in
471 eliminating vegetative cells in the posterior regions of the *Drosophila* midgut or mouse small
472 intestine, which enables *Bc/Bt* persistence. Using *Drosophila* genetic tools, we first show that
473 spores are not detected in the anterior midgut, unlike vegetative cells, which rapidly trigger
474 immune ROS production (Benguettat et al., 2018; Lee et al., 2013). Strikingly, although
475 spores germinate in the posterior midgut, there is no release of immune ROS. Immune ROS
476 are normally produced in a DUOX-dependent manner in response to uracil secretion by
477 allochthonous bacteria (Lee et al., 2013). Uracil is thought to serve as bacterial growth factor,
478 promoting proliferation (Du et al., 2016). Hence, we can assume that either *Bc/Bt* vegetative

cells in the posterior midgut do not produce uracil or the host receptor for uracil (Lee et al., 2015) is absent from the posterior midgut. Moreover, the germination of spores in the posterior midgut, through the activation of the negative regulators, amidases, dampens the production of AMPs. Consequently, the combination of the absence of ROS and the reduced levels of AMPs favor *Bc/Bt* persistence.

Why does spore germination induce only the genes encoding amidases and not those encoding AMPs in the posterior midgut? It has been shown that the Imd pathway cytosolic receptor PGRP-LE is required all along the fly midgut to activate *AMP* genes in the anterior in response to pathogenic bacteria and to upregulate the amidases PGRP-SC1 and -LB in the posterior midgut in response to commensal bacteria. The transmembrane PGRP-LC receptor is also required in cooperation with PGRP-LE in the anterior midgut to activate the expression of *AMPs* in response to pathogenic bacteria, however, PGRP-LC is dispensable in the posterior midgut (Bosco-Drayon et al., 2012; Buchon et al., 2013; Costechareyre et al., 2016; Neyen et al., 2012; Zhai et al., 2018a). Consistent with this observation, we found that only PGRP-LE is involved in response to spore ingestion. Therefore, in the posterior midgut, the germination of spores allows the activation of the Imd pathway in a PGRP-LE dependent manner, leading to the induction of *amidases* but not of *AMPs*. Hence the germination of spores of *Bc/Bt* in the posterior compartment are perceived as if they were commensal bacteria, inducing a tolerance response (Bonnay et al., 2013; Bosco-Drayon et al., 2012; Morris et al., 2016) through the induction of Amidases that in turn dampen *AMPs* expression. Our spore ingestion paradigm also reveals that when the Imd pathway is only mobilized in the posterior midgut (spores are not detected in the anterior compartment) in a PGRP-LE-dependent manner, the only response elicited is the induction of amidases, even if the ingested bacteria are non-commensal ones. Consistently, the transcription repressor Caudal has been shown to be involved in the repression of *AMP* expression specifically in the posterior midgut

(Ryu et al., 2008). Hence the midgut could be separated into two distinct immune domains: the anterior midgut is competent to fight pathogenic bacteria ingested along with the food, and the posterior midgut is immune-tolerant to sustain commensal flora. *Bc/Bt* spores have developed a strategy to hijack this physiological state for their own benefit, allowing them to escape the strong anterior immune response that would otherwise kill the germinated cells. Consistent with this model, it has been well demonstrated that the *Drosophila* posterior midgut is capable of increased cell turnover, when compared to the anterior midgut, in order to overcome the damages caused by pathogens (Apidianakis et al., 2009; Jiang et al., 2009; Marianes and Spradling, 2013; Tamamouna et al., 2020; Zhou et al., 2013), likely to compensate for a weaker innate immune response. Interestingly, our data show that spores behave similarly in the mouse small intestine, germinating preferentially in the jejunum and ileum. Moreover, the two mouse orthologs of the *Drosophila* amidases, *Pglyrp1* and *Pglyrp2* (Lee et al., 2012; Osanai et al., 2011) are also induced in the jejunum and ileum, suggesting a conserved intestinal physiological response to spore ingestion.

Unexpectedly, our work in *Drosophila* also revealed that Relish is not the sole NF-κB factor driving the innate immune response in the posterior midgut. Indeed it has been well demonstrated that Relish is absolutely required in the anterior midgut downstream of the Imd pathway to mount an efficient immune response against pathogens (Bosco-Drayon et al., 2012; Buchon et al., 2009a; Buchon et al., 2009b; Cronin et al., 2009). However, we show that in the posterior midgut, Dif intervenes to control *DptA* and *Defensin* activation, probably in cooperation with Relish, since the absence of one of the NF-κB factors is sufficient to shut down their expression. In agreement, it has been shown that during the systemic immune response, both NF-κB factors were able to form hetero- and homodimers to differentially control *AMP* genes (Han and Ip, 1999; Morris et al., 2016; Tanji et al., 2010). Similarly, Relish/Dif heterodimers likely regulate *PGRP-SC1*, since its expression is lost in either *Dif* or

529 *Rel* loss-of-function mutants. However, induction of *PGRP-LB* appears to be only under the
530 control of Relish. Finally, Dif and Relish exert opposite effects on *PGRP-SC2* expression.
531 While Rel represses its expression, Dif is required for its induction. Interestingly, it has been
532 shown that the IκB factor Pickle can bind to Relish homodimers, converting them into
533 transcriptional repressors of *AttD* expression (Morris et al., 2016). Therefore, a combination
534 of NF-κB homo- and hetero-dimers, plus the presence of specific negative regulators, fine-
535 tune the posterior immune response, limiting the level of expression of *AMPs* to enable
536 commensal flora to become established, but also unfortunately allowing some opportunistic
537 bacteria to persist. Interestingly, a role for Dif in shaping the intestinal commensal flora,
538 downstream of the Toll pathway, has recently been uncovered (Bahuguna et al., 2022). Along
539 with our results, this suggests that the Toll pathway could also be active in the posterior
540 midgut and may contribute to the immune response against pathogens.

541 Together, our data shed light on the conserved behavior and strategy of *Bc/Bt* spores to
542 escape the innate immune response in the proximal part of the small intestine, allowing them
543 to reach and germinate in the distal region. Our work also provides useful tools for further
544 investigation to understand when and how enterotoxins are produced and trigger diarrheic
545 symptoms. Our work also highlights that the persistence and load of *Bc/Bt* can be enhanced
546 and could potentially lead to more severe symptoms in immunocompromised individuals.

547

548 **AKNOWLEDGEMENT**

549 We would like to thank Bernard Charroux, François Leulier, Julien Royet, Heinrich Jasper,
550 Leopold Kurz, Mark Hanson and Bruno Lemaitre for kindly providing fly stocks. We also
551 thank Didier Lereclus for providing the pHT315 plasmid. We are grateful to Leanne Jones,
552 Raphaël Rousset, Carmelo Luci, Bernard Charroux and Bruno Lemaitre for their advice on
553 the project and the manuscript. We also thank Olivier Pierre and Anne Doye for their help for
554 the microscopy, Dorota Czerucka for mouse intestine dissection, and Olivia Benguettat for
555 her technical help. We greatly acknowledge the C3M Animal core facility. Our thanks to the

Université Côte d'Azur Office of International Scientific Visibility for English language editing of the manuscript. We also thank the Space, Environment, Risk and Resilience Academy of the Université Côte d'Azur for their financial support.

FUNDING

This work has been supported by the French government, through the UCAJEDI Investments in the Future project managed by the National Research Agency (ANR) with the reference number ANR-15-IDEX-01 and through the ANR-13-CESA-0003-01 (ImBio) and the ANR-22-CE35-0006-01 (BaDAss). This work has also been supported by the Plan ECOPHYTO II+ Axe 3 - Action 11 under the N°OFB.21.0450. AF was funded by a PhD grant from INRAE and Anses.

AUTHOR CONTRIBUTIONS

Conceptualization: S.H., L.B. and A.G.

Methodology: S.H., A.B.-B., P.M., M.-P.N.-E., G.M. and M.B.

Validation: S.H., A.B.-B., P.M., A.F., M.B., L.B. and A.G.

Formal Analysis: S.H., A.B.-B., P.M., A.F., L.B. and A.G.

Investigation: S.H., A.B.-B., P.M., M.-P.N.-E. and M.B.

Data Curation: S.H., A.B.-B., P.M., A.F., M.B. and A.G.

Writing – Original Draft: S.H. and A.G.

Writing – Review & Editing: S.H., A.B.-B., M.B., L.B. and A.G.

Visualization: S.H., L.B and A.G.

Supervision: L.B and A.G.

Project Administration: L.B. and A.G.

Funding Acquisition: M.B., R.R., L.B. and A.G.

DECLARATION OF INTERESTS

The authors declare no competing interests.

EXPERIMENTAL PROCEDURES

Bacterial strains

The two bioinsecticide strains (SA-11 and ABTS-351) were used as commercial formulations. In parallel, the strain ABTS-351 was also used after bacterial isolation and "home-made" spore production as described below. The *Btk*$^{\Delta Cry}$ strain (#4D22) was collected from the Bacillus Genetics Stock Center (www.bgsc.org) (González et al. 1982). The *Bc* (#ATCC 14579) was provided by ANSES Maisons-Alfort. *B. toyonensis* strain were selected in this work. *Erwinia carotovora carotovora 15* (*Ecc 15)* was kindly provided by Bruno Lemaitre (Basset et al., 2000). Bacterial strains were grown in LB medium at 30°C for 16 h.

Construction of SA-11$^{\Delta Cry}$

The mutant SA-11$^{\Delta Cry}$ was obtained from the WT strain SA-11, by a procedure of plasmid curing, as follows. After isolation on TSA-YE agar (Biomérieux, 18h culture at 30°C), the strain SA-11 was sub-cultured successively 3 times in 10ml of brain-heart Infusion (BHI, Oxoid) broth at 42°C with agitation, for 64, 48 and 36h respectively. The first BHI culture was inoculated from an isolated colony, and the subsequent cultures were inoculated with 100µl of the previous ones. Clones from the last culture were isolated on TSA-YE agar after serial dilution, then subcultured on the sporulating medium hydrolysate of casein tryptone (HCT) + 0.3% Glc, to select clones unable to produce crystals visible by phase contrast microscopy. The absence of plasmids carrying the *cry* genes was checked by sequencing. Briefly, the genomic DNA of SA-11$^{\Delta Cry}$ and SA-11 WT were extracted using the KingFisher cell and Tissue DNA kit (ThermoFisher) and sequenced with Illumina technology at the Institut du Cerveau et de la Moelle Epinière (ICM) platform, as previously described (Bonis et al., 2021), (SAMN23436137 and SAMN23455549, respectively). The absence of cry genes in SA-11$^{\Delta Cry}$ has been confirmed from raw reads, using KMA (Clausen et al., 2018).

Consistently, a plasmid reconstruction made with Mob-Suite (Robertson and Nash, 2018) suggested the loss of 4 plasmids in SA-11$^{\Delta Cry}$ compared with SA-11 WT.

Btk$^{\Delta Cry\text{-}GFP}$, SA-11^{GFP}, SA-11$^{\Delta CryGFP}$, *Bc*^{GFP} *and B. toyonensis*^{GFP} strains

The GFP coding sequence was inserted into the *pHT315* plasmid (bearing the erythromycin-resistant gene) (Theoduloz et al., 2003) (gift from Didier Lereclus). The *pHT315-GFP* recombinant plasmid was transfected and amplified into competent *dam*$^{-}$*/dcm*$^{-}$ *E. Coli* (NEB#C2529H) which allowed it to be demethylated. *pHT315-GFP* was then extracted and purified using either the Pureyield plasmid miniprep kit (Promega #A1223) or the QIAGEN® Plasmid Mini Kit (QIAGEN). For the extraction using the QIAGEN® Plasmid mini Kit, the DNA solution was concentrated by isopropanol precipitation following the manufacturer's recommendations and resuspended in PCR-grade water. The DNA concentrations were measured using the NanoDrop1000 spectrophotometer (Thermo Fisher Scientific).

The different strains from the *Bc* group were transfected with the *pHT315-GFP* plasmid as follows. Strains were plated on TSA-YE agar at room temperature for 48h, then subcultured in 10 ml of BHI for 18h at 30°C, after inoculation from isolated colonies. The cultures were diluted 1/100 in 100 ml BHI and incubated at 37°C under agitation until an $OD600_{nm}$ of about 0.3 was reached. Bacteria were washed in 10 ml of cold electroporation buffer (400 mM sucrose, 1mM MgCl2, phosphate-buffered saline 1X, pH 6.8) and then resuspended in 850µl of cold electroporation buffer. A hundred µl of each suspension was incubated with 250 ng of plasmid DNA in ice for 5 min, then submitted to electroporation using the MicroPulser Electroporator (Biorad, program Sta), and 2 mm electroporation cuvettes. After the addition of 0.9 ml of BHI, bacteria were incubated for 2h at 37°C and isolated on TSA-YE agar supplemented with 10 µg/ml of erythromycin. The selected clones were checked for the presence of the *GFP* gene after sequencing (SAMN23436138 and SAMN23436139, respectively), and for the expression of GFP using fluorescence microscopy.

Spore production

Strains were plated on LB-agar plates and grown overnight at 30◦C. Bacteria were grown at 30°C in HCT-agar medium (pH 7.2) containing per 1L: 5g tryptone (Oxoid), 2g casein hydrolysate (Oxoid), 15g agar, 3g glucose, and salts as previously reported in a sporulation-specific medium (Lecadet et al., 1980). After 10 days of incubation, spores were washed with 0.15% NaCl and heat-treated for 20 min at 70°C. Then cells were centrifuged at 10000g, 8°C for 20min. Spores were washed with sterile deionized water and centrifuged at 10000g, 8°C for 20min. The supernatant was discarded, and the washing was repeated once. The last pellets were taken up in 10ml and lyophilized (freeze-drying equipment model: RP2V). The numbers of spores produced were determined by estimating the CFUs on LB plates after serial dilution of lyophilized spores.

Time lapse fluorescence of SA-11$^{R/G}$ **spore germination**

SA-11$^{R/G}$ spores were placed on 1.5% agarose pads on a microscopy slide and covered with a cover glass. The use of agarose pad allowed for stabilizing spores to be achieved in the microscopy samples. The agarose pads were incubated at 37°C for 60min to accelerate spore germination process. The time lapse images were taken once every 5 minutes for 90 minutes to avoid bleaching. Images were acquired using the Zeiss LSM 880 microscope equipped with the AiryScan detector.

***Drosophila* rearing and stocks**

Flies were reared on our standard laboratory medium (Nawrot-Esposito et al., 2020) in 12h/12h light/dark cycle-controlled incubators. We used the following stocks: WT *canton S* (Bloomington #64349); W^{1118} (Bloomington #3605); Rel^{E20} (Bloomington #55714); *w;* $PGRP\text{-}LC^{\Delta E}$ (Bloomington #55713); *yw;* $PGRP\text{-}LE^{112}$ (Bloomington #33055); *w;* $PGRP\text{-}SC^{\Delta}$ (Bloomington #55724); w; $PGRP\text{-}LB^{\Delta}$ (Bloomington #55715; gift from B. Charroux); $Dredd^{F64}$ (Leulier et al., 2000) (gift from B. Charroux); $imd^{Shaddok}$ (gift from B. Charroux *); w;*

660 *Dif*^{1} (Bloomington #36559); *ΔAMP14* (gift from B. Lemaitre) (Carboni et al., 2022); *w; AttD-*
661 *Gal4 UAS-cherry* (gift from Leopold Kurz) (Tavignot et al., 2017)*; w; DptA-cherry* (gift from
662 Leopold Kurz, Bloomington #55706); *UAS-DUOX*^{RNAI} (Bloomington #38907); *UAS-REL*^{RNAI}
663 (Bloomington #33661); *UAS-PGRP-LB*^{RNAI} (Bloomington #67236); *UAS-PGRP-SC2*^{RNAI}
664 (Bloomington #56915); *w; myo1A-Gal4; tubGal80ts UAS-GFP/TM6b* (gift from Nicolas
665 Tapon) (Shaw et al., 2010). The *w; Rel*^{E20}, *Dif*^{1} homozygous viable double mutant was
666 obtained using classic mendelian genetic crosses.

667 **_Drosophila_ oral intoxication**

668 Five-six-days old virgin females *Drosophila* were reared at 25°C. For conditional expression
669 of UAS-GAL80^{ts}linked transgenes, flies were developed at room temperature, then shifted to
670 29°C for 7 days to induce transgene expression. Before intoxication, *Drosophila* females were
671 put into a new vial without medium for starvation for 2 hours at 25°C or at 29°C for UAS-
672 GAL80^{ts} flies. This allows the synchronization of food intake once in contact with the
673 contaminated medium. Ten females were transferred into a *Drosophila* narrow vial containing
674 fly medium covered with a filter disk where the spore solution was deposited. The inoculum
675 used for continuous and acute intoxication were respectively 10^{6} CFU/5 cm^{2}/fly and 10^{8}
676 CFU/5 cm^{2}/fly respectively. For the acute intoxication, *Drosophila* were fed for 30 minutes
677 with the spore inoculum, then transferred to a new sterile vial until dissection. For the
678 continuous intoxication, *Drosophila* were let in contact with the spore inoculum until the
679 dissection time. For control conditions, *Drosophila* females were fed with sterile deionized
680 water in the same conditions.

681 **Bacterial load quantification (CFU) in _Drosophila_ midgut**

682 Flies were washed first in ethanol 70% and then in PBS1X before guts dissection in PBS1X.
683 Whole midguts or split parts (anterior and posterior regions) were crushed in 200µL of LB at
684 various times post-ingestion using a micro pestle and the homogenate was serially diluted in

LB and incubated overnight at 30°C on LB agar plates. Colony counting was performed the day after.

Bacterial load quantification (CFU) on the filter disk

The filter disk was washed and vortexed in 1ml of sterile water. The homogenate was serially diluted in sterile water and incubated overnight at 30°C on LB agar plates. Colony counting was performed the day after.

Heat-treatment

The intestinal samples or the filter disk samples were heated at 75°C for 25 min to kill the germinating spores and the vegetative cells. Afterward, the spores were enumerated as described above.

***In vivo* monitoring of spore germination**

Flies were fed with *Btk* SA-11$^{R/G}$. Guts were dissected and fixed with 4% formaldehyde in PBS1X for 20min and immediately mounted in Fluoroshield-DAPI medium. Images acquisition was performed at the microscopy platform of the Institut Sophia Agrobiotech (INRAE 1355-UCA-CNRS 7254-Sophia Antipolis) with the microscope Zeiss AxioZoom V16 with an Apotome 2 and a Zeiss LSM 880 microscope equipped with the AiryScan detector. Images were analyzed using ZEN and Photoshop software and ImageJ.

RNA extraction and Real-time qPCR for *Drosophila* guts

Four biological replicates were generated for each condition. Total RNA was extracted from 10 *Drosophila* midguts using Microelute Total RNA kit (Omega Bio Tek) and dissolved in 20µl of RNase-free water. The quantity and quality of RNA were assessed using a Thermo Scientific™ NanoDrop 2000. 550ng of extracted RNA was reverse transcribed to cDNA using Qscript™. Real-time PCR was performed on AriaMX Real-Time (Agilent) in a final volume of 20µl, using the EvaGreen kit. Each experiment was independently repeated three times. Relative expression data were normalized to *RP49* and *Dp1* genes

HOCl staining with R19S

The protocol is described in (Hachfi et al., 2019).

The ethics statement for mouse model

This study was carried out in strict accordance with the guidelines of the Council of the European Union (Directive 86/609/EEC) regarding the protection of animals used for experimental and other scientific purposes. The protocol was approved by the Institutional Animal Care and Use Committee on the Ethics of Animal Experiments of Nice, France (APAFIS#18923-2019012512125055 v3).

Mice

Female Balb/c mice (7 weeks of age) were used. The mice were matched by age with a control group. The mice were kept in animal house facilities with 12:12-h light/dark cycles in standard animal cages and fed with a standard pellet diet, as well as a plastic bottle. Mice were acclimatized to these conditions for 1 week before entering the study.

Mice oral administration

Balb/c mice (7 weeks, female) were divided into two groups (n=5-10). There was no significant difference in body weight between the groups. Mice received 200µl of bacterial suspension or sterile PBS1X. The bacterial suspension was prepared by dissolving spores/bacterial at a concentration of 10^8 CFU/mouse. All mice were transferred to freshly sterilized cages every day.

Bacterial load quantification (CFU) in mice small intestines

At the time of dissection, Mice received freshly prepared Ketamine-Xylazine (10mg/ml)-10mg/ml) mixture doses. The anesthetic mixture was injected intraperitoneal IP. Blood was collected from a tail vein sampling. Then, mice were euthanized. Duodenum, jejunum, ileum were sampled, weighed, and crushed in 1ml of sterile PBS1X using the precellys lysing kits

734 CK14 (Bertin Technologies) The homogenate was serially diluted in PBS1Xx and incubated
735 overnight at 30°C on LB agar plates. Colony counting was performed the day after.

736 ***In-vivo* monitoring of spore germination in mice small intestines**

737 Mice fasted for 48h SA-11^{GFP}spores suspension per gavage at a concentration of 10^8
738 CFU/mouse. Guts were dissected and immediately visualized with PhotonIMAGER Optima
739 (Biospace Lab, Nesles-la-Vall□e, France). The data was analysed using M3 Vision software
740 (Biospace Lab, Nesles-la-Vall□e, France) version 1.1.2.26170 and Fuji software.

741 **RNA extraction and RT-qPCR for mice guts**

742 One centimeter of intestinal tissue (duodenum, jejunum, or ileum) was homogenized in 2mL
743 tubes containing 300µl Trizol using the Precellys® system. The duodenum part was taken
744 directly after the stomach, the jejunum part was taken in the middle, and the ileum was the
745 distal part near the cecum. After extraction with chloroform, precipitation with isopropanol
746 and washings with 70% ethanol, and extracted RNA was resuspended in 50µL of sterile
747 distilled water. cDNA synthesis was performed with Applied Biosystems™ Kit (Thermo
748 Fisher Scientific). Gene expression was analyzed by quantitative reverse transcription PCR
749 (qRT-PCR) analysis on a QuantStudio™ 5 Real-Time PCR System (Thermo Fisher
750 Scientific) and normalized to endogenous control gene mGUS. Gene expression is depicted as
751 relative mRNA amounts (relative quantities (RQ) after normalization to the expression of
752 endogenous control gene mGUS calculated using delta/delta Ct method with the software
753 provided by QuantStudio™ 5 Real-Time PCR System.

754 **Quantification and statistical analysis**

755 Statistical analyses were performed using GraphPad Prism v.7.00 or Microsoft Excel
756 softwares. Data are presented as mean and SEM. For all comparisons throughout our study,
757 we performed Mann Whitney's test or Student's t-tests as specified on each figure legends.
758 *p≤0.05, **p≤ 0.01, ***p≤0.001, ns = non-significant.

REFERENCES

Apidianakis, Y., Pitsouli, C., Perrimon, N., and Rahme, L. (2009). Synergy between bacterial infection and genetic predisposition in intestinal dysplasia. Proc Natl Acad Sci U S A *106*, 20883-20888. Epub 22009 Nov 20823.

Bahuguna, S., Atilano, M., Glittenberg, M., Lee, D., Arora, S., Wang, L., Zhou, J., Redhai, S., Boutros, M., and Ligoxygakis, P. (2022). Bacterial recognition by PGRP-SA and downstream signalling by Toll/DIF sustain commensal gut bacteria in Drosophila. PLoS Genet *18*, e1009992.

Barbosa, T. M., Serra, C. R., La Ragione, R. M., Woodward, M. J., and Henriques, A. O. (2005). Screening for bacillus isolates in the broiler gastrointestinal tract. Appl Environ Microbiol *71*, 968-978. doi: 910.1128/AEM.1171.1122.1968-1978.2005.

Basset, A., Khush, R. S., Braun, A., Gardan, L., Boccard, F., Hoffmann, J. A., and Lemaitre, B. (2000). The phytopathogenic bacteria Erwinia carotovora infects Drosophila and activates an immune response. Proc Natl Acad Sci U S A *97*, 3376-3381.

Benguettat, O., Jneid, R., Soltys, J., Loudhaief, R., Brun-Barale, A., Osman, D., and Gallet, A. (2018). The DH31/CGRP enteroendocrine peptide triggers intestinal contractions favoring the elimination of opportunistic bacteria. PLoS Pathog *14*, e1007279. doi: 1007210.1001371/journal.ppat.1007279. eCollection 1002018 Sep.

Berthold-Pluta, A., Pluta, A., and Garbowska, M. (2015). The effect of selected factors on the survival of Bacillus cereus in the human gastrointestinal tract. Microb Pathog *82:7-14.*, 10.1016/j.micpath.2015.1003.1015. Epub 2015 Mar 1017.

Biggel, M., Etter, D., Corti, S., Brodmann, P., Stephan, R., Ehling-Schulz, M., and Johler, S. (2021). Whole Genome Sequencing Reveals Biopesticidal Origin of Bacillus thuringiensis in Foods. Front Microbiol *12*, 775669.

Bonfini, A., Liu, X., and Buchon, N. (2016). From pathogens to microbiota: How Drosophila intestinal stem cells react to gut microbes. S0145-0305X(0116)30032-30035. doi: 30010.31016/j.dci.32016.30002.30008.

Bonis, M., Felten, A., Pairaud, S., Dijoux, A., Maladen, V., Mallet, L., Radomski, N., Duboisset, A., Arar, C., Sarda, X., *et al.* (2021). Comparative phenotypic, genotypic and genomic analyses of Bacillus thuringiensis associated with foodborne outbreaks in France. PLoS One *16*, e0246885.

Bonnay, F., Cohen-Berros, E., Hoffmann, M., Kim, S. Y., Boulianne, G. L., Hoffmann, J. A., Matt, N., and Reichhart, J. M. (2013). big bang gene modulates gut immune tolerance in Drosophila. Proc Natl Acad Sci U S A *110*, 2957-2962.

Bosco-Drayon, V., Poidevin, M., Boneca, I. G., Narbonne-Reveau, K., Royet, J., and Charroux, B. (2012). Peptidoglycan sensing by the receptor PGRP-LE in the Drosophila gut induces immune responses to infectious bacteria and tolerance to microbiota. Cell Host Microbe *12*, 153-165.

Buchon, N., Broderick, N. A., Chakrabarti, S., and Lemaitre, B. (2009a). Invasive and indigenous microbiota impact intestinal stem cell activity through multiple pathways in Drosophila. Genes Dev *23*, 2333-2344. doi: 2310.1101/gad.1827009.

Buchon, N., Broderick, N. A., Poidevin, M., Pradervand, S., and Lemaitre, B. (2009b). Drosophila intestinal response to bacterial infection: activation of host defense and stem cell proliferation. Cell Host Microbe *5*, 200-211. doi: 210.1016/j.chom.2009.1001.1003.

Buchon, N., Osman, D., David, F. P., Fang, H. Y., Boquete, J. P., Deplancke, B., and Lemaitre, B. (2013). Morphological and molecular characterization of adult midgut compartmentalization in Drosophila. Cell Rep *3*, 1725-1738. doi: 1710.1016/j.celrep.2013.1704.1001. Epub 2013 May 1722.

807 Capo, F., Wilson, A., and Di Cara, F. (2019). The Intestine of Drosophila melanogaster: An
808 Emerging Versatile Model System to Study Intestinal Epithelial Homeostasis and Host-
809 Microbial Interactions in Humans. Microorganisms *7(9).* microorganisms7090336. doi:
810 7090310.7093390/microorganisms7090336.
811 Carboni, A. L., Hanson, M. A., Lindsay, S. A., Wasserman, S. A., and Lemaitre, B. (2021).
812 Cecropins contribute to Drosophila host defense against a subset of fungal and Gram-negative
813 bacterial infection. Genetics *220*.
814 Carboni, A. L., Hanson, M. A., Lindsay, S. A., Wasserman, S. A., and Lemaitre, B. (2022).
815 Cecropins contribute to Drosophila host defense against a subset of fungal and Gram-negative
816 bacterial infection. Genetics *220*.
817 Carroll, L. M., Cheng, R. A., Wiedmann, M., and Kovac, J. (2021). Keeping up with the
818 Bacillus cereus group: taxonomy through the genomics era and beyond. Crit Rev Food Sci
819 Nutr, 1-26.
820 Carroll, L. M., Wiedmann, M., and Kovac, J. (2020). Proposal of a Taxonomic Nomenclature
821 for the Bacillus cereus Group Which Reconciles Genomic Definitions of Bacterial Species
822 with Clinical and Industrial Phenotypes. mBio *11*.
823 Casula, G., and Cutting, S. M. (2002). Bacillus probiotics: spore germination in the
824 gastrointestinal tract. Appl Environ Microbiol *68*, 2344-2352.
825 Ceuppens, S., Uyttendaele, M., Drieskens, K., Heyndrickx, M., Rajkovic, A., Boon, N., and
826 Van de Wiele, T. (2012a). Survival and germination of Bacillus cereus spores without
827 outgrowth or enterotoxin production during in vitro simulation of gastrointestinal transit. Appl
828 Environ Microbiol *78*, 7698-7705. doi: 7610.1128/AEM.02142-02112. Epub 02012 Aug
829 02124.
830 Ceuppens, S., Uyttendaele, M., Drieskens, K., Rajkovic, A., Boon, N., and Wiele, T. V.
831 (2012b). Survival of Bacillus cereus vegetative cells and spores during in vitro simulation of
832 gastric passage. J Food Prot *75*, 690-694. doi: 610.4315/0362-4028X.JFP-4311-4481.
833 Ceuppens, S., Uyttendaele, M., Hamelink, S., Boon, N., and Van de Wiele, T. (2012c).
834 Inactivation of Bacillus cereus vegetative cells by gastric acid and bile during in vitro
835 gastrointestinal transit. Gut Pathog *4*, 11. doi: 10.1186/1757-4749-1184-1111.
836 Chakrabarti, S., Liehl, P., Buchon, N., and Lemaitre, B. (2012). Infection-induced host
837 translational blockage inhibits immune responses and epithelial renewal in the Drosophila gut.
838 Cell Host Microbe *12*, 60-70. doi: 10.1016/j.chom.2012.1006.1001.
839 Charroux, B., Capo, F., Kurz, C. L., Peslier, S., Chaduli, D., Viallat-Lieutaud, A., and Royet,
840 J. (2018). Cytosolic and Secreted Peptidoglycan-Degrading Enzymes in Drosophila
841 Respectively Control Local and Systemic Immune Responses to Microbiota. Cell Host
842 Microbe *23*, 215-228.e214.
843 Chen, X., Lee, K. A., Ha, E. M., Lee, K. M., Seo, Y. Y., Choi, H. K., Kim, H. N., Kim, M. J.,
844 Cho, C. S., Lee, S. Y., *et al.* (2011). A specific and sensitive method for detection of
845 hypochlorous acid for the imaging of microbe-induced HOCl production. Chem Commun
846 (Camb) *47*, 4373-4375. doi: 4310.1039/c4371cc10589b. Epub 12011 Mar 10514.
847 Clausen, P., Aarestrup, F. M., and Lund, O. (2018). Rapid and precise alignment of raw reads
848 against redundant databases with KMA. BMC Bioinformatics *19*, 307.
849 Clavel, T., Carlin, F., Lairon, D., Nguyen-The, C., and Schmitt, P. (2004). Survival of
850 Bacillus cereus spores and vegetative cells in acid media simulating human stomach. J Appl
851 Microbiol *97*, 214-219. doi: 210.1111/j.1365-2672.2004.02292.x.
852 Costechareyre, D., Capo, F., Fabre, A., Chaduli, D., Kellenberger, C., Roussel, A., Charroux,
853 B., and Royet, J. (2016). Tissue-Specific Regulation of Drosophila NF-x03BA;B Pathway
854 Activation by Peptidoglycan Recognition Protein SC. J Innate Immun *8*, 67-80. doi:
855 10.1159/000437368. Epub 000432015 Oct 000437330.

856 Cronin, S. J., Nehme, N. T., Limmer, S., Liegeois, S., Pospisilik, J. A., Schramek, D.,
857 Leibbrandt, A., Simoes Rde, M., Gruber, S., Puc, U., *et al.* (2009). Genome-wide RNAi
858 screen identifies genes involved in intestinal pathogenic bacterial infection. Science *325*, 340-
859 343. doi: 310.1126/science.1173164. Epub 1172009 Jun 1173111.
860 Dietrich, R., Jessberger, N., Ehling-Schulz, M., Märtlbauer, E., and Granum, P. E. (2021).
861 The Food Poisoning Toxins of Bacillus cereus. Toxins (Basel) *13*.
862 Du, E. J., Ahn, T. J., Kwon, I., Lee, J. H., Park, J. H., Park, S. H., Kang, T. M., Cho, H., Kim,
863 T. J., Kim, H. W., *et al.* (2016). TrpA1 Regulates Defecation of Food-Borne Pathogens under
864 the Control of the Duox Pathway. PLoS Genet *12*, e1005773. doi:
865 1005710.1001371/journal.pgen.1005773. eCollection 1002016 Jan.
866 Duport, C., Thomassin, S., Bourel, G., and Schmitt, P. (2004). Anaerobiosis and low specific
867 growth rates enhance hemolysin BL production by Bacillus cereus F4430/73. Arch Microbiol
868 *182*, 90-95.
869 Duport, C., Zigha, A., Rosenfeld, E., and Schmitt, P. (2006). Control of enterotoxin gene
870 expression in Bacillus cereus F4430/73 involves the redox-sensitive ResDE signal
871 transduction system. J Bacteriol *188*, 6640-6651.
872 EFSA, and ECDC (2018). The European Union summary report on trends and sources of
873 zoonoses, zoonotic agents and food-borne outbreaks in 2017. EFSA Journal *16*, e05500.
874 EFSA BIOHAZ (2016). Risks for public health related to the presence of Bacillus cereus and
875 other Bacillus spp. including Bacillus thuringiensis in foodstuffs. EFSA Journal *14*, e04524.
876 Ehling-Schulz, M., Lereclus, D., and Koehler, T. M. (2019). The Bacillus cereus Group:
877 Bacillus Species with Pathogenic Potential. Microbiol Spectr *7(3)*.
878 10.1128/microbiolspec.GPP1123-0032-2018.
879 Glasset, B., Herbin, S., Guillier, L., Cadel-Six, S., Vignaud, M. L., Grout, J., Pairaud, S.,
880 Michel, V., Hennekinne, J. A., Ramarao, N., and Brisabois, A. (2016). Bacillus cereus-
881 induced food-borne outbreaks in France, 2007 to 2014: epidemiology and genetic
882 characterisation. Euro Surveill *21(48)*. 30413. doi: 30410.32807/31560-
883 37917.ES.32016.30421.30448.30413.
884 Guo, L., Karpac, J., Tran, S. L., and Jasper, H. (2014). PGRP-SC2 promotes gut immune
885 homeostasis to limit commensal dysbiosis and extend lifespan. Cell *156*, 109-122. doi:
886 110.1016/j.cell.2013.1012.1018.
887 Hachfi, S., Benguettat, O., and Gallet, A. (2019). Hypochlorous Acid Staining with R19-S in
888 the Drosophila Intestine upon Ingestion of Opportunistic Bacteria. Bio-protocol *9*, e3246.
889 Han, Z. S., and Ip, Y. T. (1999). Interaction and specificity of Rel-related proteins in
890 regulating Drosophila immunity gene expression. J Biol Chem *274*, 21355-21361.
891 Hanson, M. A., Dostálová, A., Ceroni, C., Poidevin, M., Kondo, S., and Lemaitre, B. (2019).
892 Synergy and remarkable specificity of antimicrobial peptides in vivo using a systematic
893 knockout approach. eLife *8*, e44341.
894 Hedengren, M., Asling, B., Dushay, M. S., Ando, I., Ekengren, S., Wihlborg, M., and
895 Hultmark, D. (1999). Relish, a central factor in the control of humoral but not cellular
896 immunity in Drosophila. Mol Cell *4*, 827-837.
897 Jensen, G. B., Larsen, P., Jacobsen, B. L., Madsen, B., Smidt, L., and Andrup, L. (2002).
898 Bacillus thuringiensis in fecal samples from greenhouse workers after exposure to B.
899 thuringiensis-based pesticides. Appl Environ Microbiol *68*, 4900-4905.
900 Jiang, H., Patel, P. H., Kohlmaier, A., Grenley, M. O., McEwen, D. G., and Edgar, B. A.
901 (2009). Cytokine/Jak/Stat signaling mediates regeneration and homeostasis in the Drosophila
902 midgut. Cell *137*, 1343-1355. doi: 1310.1016/j.cell.2009.1305.1014.
903 Johler, S., Kalbhenn, E. M., Heini, N., Brodmann, P., Gautsch, S., Bagcioglu, M., Contzen,
904 M., Stephan, R., and Ehling-Schulz, M. (2018). Enterotoxin Production of Bacillus

905 thuringiensis Isolates From Biopesticides, Foods, and Outbreaks. Front Microbiol *9:1915.*,
906 10.3389/fmicb.2018.01915. eCollection 02018.
907 Jovanovic, J., Ornelis, V. F. M., Madder, A., and Rajkovic, A. (2021). Bacillus cereus food
908 intoxication and toxicoinfection. Compr Rev Food Sci Food Saf *20*, 3719-3761.
909 Kaneko, T., Yano, T., Aggarwal, K., Lim, J. H., Ueda, K., Oshima, Y., Peach, C., Erturk-
910 Hasdemir, D., Goldman, W. E., Oh, B. H., *et al.* (2006). PGRP-LC and PGRP-LE have
911 essential yet distinct functions in the drosophila immune response to monomeric DAP-type
912 peptidoglycan. Nat Immunol *7*, 715-723.
913 Kenagy, G. J., and Hoyt, D. F. (1979). Reingestion of feces in rodents and its daily
914 rhythmicity. Oecologia *44*, 403-409.
915 Kim, S. H., and Lee, W. J. (2014). Role of DUOX in gut inflammation: lessons from
916 Drosophila model of gut-microbiota interactions. Front Infect Microbiol *3*, 116.
917 Lee, J., Geddes, K., Streutker, C., Philpott, D. J., and Girardin, S. E. (2012). Role of mouse
918 peptidoglycan recognition protein PGLYRP2 in the innate immune response to Salmonella
919 enterica serovar Typhimurium infection in vivo. Infect Immun *80*, 2645-2654.
920 Lee, K. A., Kim, B., Bhin, J., Kim do, H., You, H., Kim, E. K., Kim, S. H., Ryu, J. H.,
921 Hwang, D., and Lee, W. J. (2015). Bacterial Uracil Modulates Drosophila DUOX-Dependent
922 Gut Immunity via Hedgehog-Induced Signaling Endosomes. Cell Host Microbe *17*, 191-204.
923 doi: 110.1016/j.chom.2014.1012.1012. Epub 2015 Jan 1029.
924 Lee, K. A., Kim, S. H., Kim, E. K., Ha, E. M., You, H., Kim, B., Kim, M. J., Kwon, Y., Ryu,
925 J. H., and Lee, W. J. (2013). Bacterial-derived uracil as a modulator of mucosal immunity and
926 gut-microbe homeostasis in Drosophila. Cell *153*, 797-811. doi:
927 710.1016/j.cell.2013.1004.1009.
928 Leulier, F., Rodriguez, A., Khush, R. S., Abrams, J. M., and Lemaitre, B. (2000). The
929 Drosophila caspase Dredd is required to resist gram-negative bacterial infection. EMBO Rep
930 *1*, 353-358.
931 Loudhaief, R., Brun-Barale, A., Benguettat, O., Nawrot-Esposito, M. P., Pauron, D., Amichot,
932 M., and Gallet, A. (2017). Apoptosis restores cellular density by eliminating a physiologically
933 or genetically induced excess of enterocytes in the Drosophila midgut. Development *144*,
934 808-819. doi: 810.1242/dev.142539.
935 Manfruelli, P., Reichhart, J. M., Steward, R., Hoffmann, J. A., and Lemaitre, B. (1999). A
936 mosaic analysis in Drosophila fat body cells of the control of antimicrobial peptide genes by
937 the Rel proteins Dorsal and DIF. Embo j *18*, 3380-3391.
938 Marianes, A., and Spradling, A. C. (2013). Physiological and stem cell compartmentalization
939 within the Drosophila midgut. Elife *2:e00886.*, 10.7554/eLife.00886.
940 Meng, X., Khanuja, B. S., and Ip, Y. T. (1999). Toll receptor-mediated Drosophila immune
941 response requires Dif, an NF-kappaB factor. Genes Dev *13*, 792-797.
942 Miller, B. M., Liou, M. J., Lee, J. Y., and Bäumler, A. J. (2021). The longitudinal and cross-
943 sectional heterogeneity of the intestinal microbiota. Curr Opin Microbiol *63*, 221-230.
944 Morris, O., Liu, X., Domingues, C., Runchel, C., Chai, A., Basith, S., Tenev, T., Chen, H.,
945 Choi, S., Pennetta, G., *et al.* (2016). Signal Integration by the IκB Protein Pickle Shapes
946 Drosophila Innate Host Defense. Cell Host Microbe *20*, 283-295.
947 Nawrot-Esposito, M. P., Babin, A., Pasco, M., Poirié, M., Gatti, J. L., and Gallet, A. (2020).
948 Bacillus thuringiensis Bioinsecticides Induce Developmental Defects in Non-Target
949 Drosophila melanogaster Larvae. Insects *11*.
950 Neyen, C., Poidevin, M., Roussel, A., and Lemaitre, B. (2012). Tissue- and ligand-specific
951 sensing of gram-negative infection in drosophila by PGRP-LC isoforms and PGRP-LE. J
952 Immunol *189*, 1886-1897. doi: 1810.4049/jimmunol.1201022. Epub 1202012 Jul 1201026.
953 Oliveira-Filho, E. C., Oliveira, R. S., Lopes, M. C., Ramos, F. R., Grisolia, C. K., Alves, R.
954 T., and Monnerat, R. G. (2009). Toxicity assessment and clearance of Brazilian microbial pest

955 control agents in mice. Bull Environ Contam Toxicol *83*, 570-574. doi: 510.1007/s00128-
956 00009-09817-00122. Epub 02009 Jul 00129.
957 Osanai, A., Sashinami, H., Asano, K., Li, S. J., Hu, D. L., and Nakane, A. (2011). Mouse
958 peptidoglycan recognition protein PGLYRP-1 plays a role in the host innate immune response
959 against Listeria monocytogenes infection. Infect Immun *79*, 858-866.
960 Osman, D., Buchon, N., Chakrabarti, S., Huang, Y. T., Su, W. C., Poidevin, M., Tsai, Y. C.,
961 and Lemaitre, B. (2012). Autocrine and paracrine unpaired signaling regulate intestinal stem
962 cell maintenance and division. J Cell Sci *125*, 5944-5949. doi: 5910.1242/jcs.113100. Epub
963 112012 Oct 113104.
964 Paredes, J. C., Welchman, D. P., Poidevin, M., and Lemaitre, B. (2011). Negative regulation
965 by amidase PGRPs shapes the Drosophila antibacterial response and protects the fly from
966 innocuous infection. Immunity *35*, 770-779. doi: 710.1016/j.immuni.2011.1009.1018.
967 Petersen, U. M., Björklund, G., Ip, Y. T., and Engström, Y. (1995). The dorsal-related
968 immunity factor, Dif, is a sequence-specific trans-activator of Drosophila Cecropin gene
969 expression. Embo j *14*, 3146-3158.
970 Robertson, J., and Nash, J. H. E. (2018). MOB-suite: software tools for clustering,
971 reconstruction and typing of plasmids from draft assemblies. Microb Genom *4*.
972 Rolny, I. S., Minnaard, J., Racedo, S. M., and Pérez, P. F. (2014). Murine model of Bacillus
973 cereus gastrointestinal infection. J Med Microbiol *63*, 1741-1749.
974 Rosetto, M., Engström, Y., Baldari, C. T., Telford, J. L., and Hultmark, D. (1995). Signals
975 from the IL-1 receptor homolog, Toll, can activate an immune response in a Drosophila
976 hemocyte cell line. Biochem Biophys Res Commun *209*, 111-116.
977 Royet, J., and Charroux, B. (2013). Mechanisms and consequence of bacteria detection by the
978 Drosophila gut epithelium. Gut *4*, 259-263. doi: 210.4161/gmic.24386. Epub 22013 Apr
979 24312.
980 Ryu, J. H., Kim, S. H., Lee, H. Y., Bai, J. Y., Nam, Y. D., Bae, J. W., Lee, D. G., Shin, S. C.,
981 Ha, E. M., and Lee, W. J. (2008). Innate immune homeostasis by the homeobox gene caudal
982 and commensal-gut mutualism in Drosophila. Science *319*, 777-782. doi:
983 710.1126/science.1149357. Epub 1142008 Jan 1149324.
984 Santé publique France (2019). Surveillance des toxi-infections alimentaires collectives -
985 Données de la déclaration obligatoire 2018 (https://www.santepubliquefrance.fr/).
986 Setlow, P. (2014). Spore Resistance Properties. Microbiol Spectr *2(5)*.
987 10.1128/microbiolspec.TBS-0003-2012.
988 Shanbhag, S., and Tripathi, S. (2009). Epithelial ultrastructure and cellular mechanisms of
989 acid and base transport in the Drosophila midgut. J Exp Biol *212*, 1731-1744. doi:
990 1710.1242/jeb.029306.
991 Shaw, R. L., Kohlmaier, A., Polesello, C., Veelken, C., Edgar, B. A., and Tapon, N. (2010).
992 The Hippo pathway regulates intestinal stem cell proliferation during Drosophila adult midgut
993 regeneration. Development *137*, 4147-4158. doi: 4110.1242/dev.052506. Epub 052010 Nov
994 052510.
995 Tam, N. K., Uyen, N. Q., Hong, H. A., Duc le, H., Hoa, T. T., Serra, C. R., Henriques, A. O.,
996 and Cutting, S. M. (2006). The intestinal life cycle of Bacillus subtilis and close relatives. J
997 Bacteriol *188*, 2692-2700.
998 Tamamouna, V., Panagi, M., Theophanous, A., Demosthenous, M., Michail, M.,
999 Papadopoulou, M., Teloni, S., Pitsouli, C., and Apidianakis, Y. (2020). Evidence of two types
1000 of balance between stem cell mitosis and enterocyte nucleus growth in the Drosophila midgut.
1001 Development *147*.
1002 Tanji, T., Yun, E. Y., and Ip, Y. T. (2010). Heterodimers of NF-kappaB transcription factors
1003 DIF and Relish regulate antimicrobial peptide genes in Drosophila. Proc Natl Acad Sci U S A
1004 *107*, 14715-14720.

Tavignot, R., Chaduli, D., Djitte, F., Charroux, B., and Royet, J. (2017). Inhibition of a NF-κB/Diap1 Pathway by PGRP-LF Is Required for Proper Apoptosis during Drosophila Development. PLoS Genet *13*, e1006569.

Theoduloz, C., Vega, A., Salazar, M., González, E., and Meza-Basso, L. (2003). Expression of a Bacillus thuringiensisdelta-endotoxin cry1Ab gene in Bacillus subtilis and Bacillus licheniformis strains that naturally colonize the phylloplane of tomato plants (Lycopersicon esculentum, Mills). J Appl Microbiol *94*, 375-381.

Tzou, P., Ohresser, S., Ferrandon, D., Capovilla, M., Reichhart, J. M., Lemaitre, B., Hoffmann, J. A., and Imler, J. L. (2000). Tissue-specific inducible expression of antimicrobial peptide genes in Drosophila surface epithelia. Immunity *13*, 737-748.

van der Voort, M., and Abee, T. (2009). Transcriptional regulation of metabolic pathways, alternative respiration and enterotoxin genes in anaerobic growth of Bacillus cereus ATCC 14579. J Appl Microbiol *107*, 795-804.

Vodovar, N., Vinals, M., Liehl, P., Basset, A., Degrouard, J., Spellman, P., Boccard, F., and Lemaitre, B. (2005). Drosophila host defense after oral infection by an entomopathogenic Pseudomonas species. Proc Natl Acad Sci U S A *102*, 11414-11419. Epub 12005 Aug 11411.

Wilcks, A., Smidt, L., Bahl, M. I., Hansen, B. M., Andrup, L., Hendriksen, N. B., and Licht, T. R. (2008). Germination and conjugation of Bacillus thuringiensis subsp. israelensis in the intestine of gnotobiotic rats. J Appl Microbiol *104*, 1252-1259. Epub 2007 Nov 1227.

Zhai, Z., Boquete, J. P., and Lemaitre, B. (2018a). Cell-Specific Imd-NF-kappaB Responses Enable Simultaneous Antibacterial Immunity and Intestinal Epithelial Cell Shedding upon Bacterial Infection. Immunity *48*, 897-910 e897.

Zhai, Z., Huang, X., and Yin, Y. (2018b). Beyond immunity: The Imd pathway as a coordinator of host defense, organismal physiology and behavior. Dev Comp Immunol *83*, 51-59.

Zhou, F., Rasmussen, A., Lee, S., and Agaisse, H. (2013). The UPD3 cytokine couples environmental challenge and intestinal stem cell division through modulation of JAK/STAT signaling in the stem cell microenvironment. Dev Biol *373*, 383-393. doi: 310.1016/j.ydbio.2012.1010.1023. Epub 2012 Oct 1027.

Zigha, A., Rosenfeld, E., Schmitt, P., and Duport, C. (2006). Anaerobic cells of Bacillus cereus F4430/73 respond to low oxidoreduction potential by metabolic readjustments and activation of enterotoxin expression. Arch Microbiol *185*, 222-233.

FIGURE LEGENDS

Figure 1. Spores of the *Bacillus cereus* group persist in the *Drosophila* intestine.

(**A)** Experimental setup to assess bacterial load after a continuous ingestion of spores.

(B) Bacterial loads of dissected midguts after continuous ingestion of spores from *Btk* or *Bc* strains. The vertical axis indicates the median number of colony-forming units (CFUs) per midgut of at least three independent experiments. Error bars correspond to the SEM.

(**C)** Experimental setup to assess bacterial load after an acute ingestion of spores. Flies are in contact with the contaminated medium for 30 minutes and then transferred to fresh vial devoid of spores.

(D) Bacterial loads of dissected midguts after acute ingestion of spores from *Btk* or *Bc* strains. The vertical axis indicates the median number of CFUs per midgut of at least four independent experiments. Error bars correspond to the SEM.

(E) Bacterial loads in split *Drosophila* midguts after acute intoxication with *Btk* (SA-11) or *Bc* spores. Error bars correspond to the SEM of at least three independent experiments. Mann-Whitney tests were applied. Asterisks represent a statistically significant differences between bacterial loads in the anterior and the posterior midguts: **p < 0.01, *p < 0.05

Figure 2: SA-11 spores germinate preferentially in *Drosophila* posterior midgut.

(A) Time-lapse images of SA-11$^{R/G}$ spores during germination.

(B) Monitoring of SA-11$^{R/G}$ germination *in vivo* in *Drosophila* midgut 4 h post-spore-ingestion.

(C) Plots of the average fluorescence intensity (represented as mean gray value) of SA-11$^{R/G}$ germination measured along the *Drosophila* midgut presented in (B). For all plot analyses of average fluorescence shown in this paper, the red line represents the average of the spore fluorescence (Red) and the green line represents the average fluorescence of vegetative cells (GFP).

(D-E) Bacterial load of SA-11 or *Bc* in anterior (D) and posterior (E) *Drosophila* midguts. Green bars (non-heated samples) represent the whole SA-11 or *Bc* bacterial loads (spores and vegetative cells). Red bars (heated samples) represent the proportion of spore loads. Data represent the mean ± SEM of at least five independent experiments.

Figure 3: *Bacillus cereus* spores do not trigger midgut innate immune response

(A) ROS monitoring after acute feeding with SA-11 spores or vegetative cells. ROS production in the midgut is visualized by the HOCl-specific R19S probe (orange). DAPI (blue) marks the nuclei.

(B) SA-11 loads in midguts knocked down for the expression of *Duox* in enterocytes 0.5 or 4 hours after acute feeding with vegetative cells or spores. The horizontal axis indicates the median number of CFUs per midgut of at least three independent experiments. Error bars correspond to the SEM.

(C) *DptA-Cherry* expression (red) in the R1 midgut region (upper panel) and in the R5 midgut region (bottom panel) of *Drosophila* fed for 30 minutes with H_2O, *Ecc15*, SA-11 vegetative cells (Bt_{vg}) or SA-11 spores (Bt_{sp}) and observed 24 hours later. Measured quantities are shown on the right graphs. The results are given as the relative expression compared with the control (H_2O). Data represent means ± SEM of at least three independent experiments.

(D) *AttD-Gal4 UAS-Cherry* expression (red) in the R1 midgut region (upper panel) and in R4 midgut region (bottom panel) of *Drosophila* fed for 30 minutes with H_2O, *Ecc15*, SA-11 vegetative cells (Bt_{vg}), or SA-11 spores (Bt_{sp}) and observed 24 hours later. Measured quantities are shown on the right graphs. The results are given as the relative expression compared with the control (H_2O). Data represent means ± SEM of at least three independent experiments.

(E) qRT-PCR analyses of *AMP* expression in midgut upon acute feeding with SA-11 or *Bc* spores. UC corresponds to flies fed with water. For RT-qPCR results, mRNA levels in unchallenged wild-type flies were set to 100 and all other values were expressed as a percentage of this value. RT-qPCR results are shown as mean ± SEM from 10 female flies per genotype from at least three independent experiments.

(F) Bacterial load in the midguts of ΔAMP^{14} mutant flies 0.5 or 4 hours after acute feeding with SA-11 spores. The vertical axis indicates the median number of CFUs per midgut. Error bars correspond to the SEM.

(G) Representative confocal images showing SA-$11^{R/G}$ spore germination in the anterior and posterior midgut of WT (Canton S) and ΔAMP^{14} mutant flies 6 hours after acute feeding with spores. DAPI (blue) marks the nuclei. Spores are in red, vegetative cells in green. The yellow fluorescence corresponds to germinating spores (see Figure 2A).

The Mann-Whitney test was applied in B, C ,D and F. Student's t-tests were used to analyze data in E. *p≤0.05, **p≤ 0.01, ***p≤0.001, ns = non-significant.

Figure 4: Amidases are involved in *Bt/Bc* persistence

(A) qRT-PCR analyses of *amidase* expressions in midguts upon SA-11 or *Bc* spore acute feeding. UC corresponds to flies fed with water. Results are shown as mean ± SEM of 10 flies from at least three independent experiments.

(B) Bacterial load in midguts of *PGRP-SC1/2*$^{\Delta}$ double mutant or *PGRP-LB*$^{\Delta E}$ mutant 0.5 or 120 hours after SA-11 acute feeding with spores.

(C) Representative confocal images showing SA-11$^{R/G}$ spore germination in the anterior and posterior midgut of WT (Canton S), *PGRP-SC1/2*$^{\Delta}$ double mutant or *PGRP-LB*$^{\Delta E}$ mutant flies 6 hours after spore acute feeding. DAPI (blue) marks the nuclei. Spores are in red, vegetative cells in green. The yellow fluorescence corresponds to germinating spores (see Figure 2A).

(D) qRT-PCR analyses of *AMP* expressions in midguts of *PGRP-SC1/2*$^{\Delta}$ mutants following acute feeding with SA-11 spores. UC corresponds to *PGRP-SC1/2*$^{\Delta}$ flies fed with water. mRNA levels in unchallenged *PGRP-SC1/2*$^{\Delta}$ flies were set to 100 and all other values were expressed as a percentage of this value.

(E) SA-11 load in midguts of flies silenced for *PGRP-SC2* or *PGRP-LB* specifically in enterocytes (using the *myo1A*^{ts} driver) 0.5 or 120 hours after acute feeding with spores.

Student's t-tests were used to analyze data in A and D. The Mann-Whitney test was used to analyze data in B and E. *p≤0.05, **p≤ 0.01, ***p≤0.001, ns = non-significant.

Figure 5: Imd pathway components but not the transcription factor (Relish) are involved in *Bacillus cereus* persistence

(A-C) SA-11 bacterial load in midguts of homozygous mutants for different components of the Imd pathway: *PGRP-LE*^{112} *and PGRP-LC*$^{\Delta}$ (A), *Imd*^{shaddok} and *Dredd*^{F64} (B), *Rel*^{E20} (C) 0.5 or 120 hours after acute feeding with spores.

(D) SA-11 bacterial loads in midguts of flies silenced for *Relish* expression in the enterocytes (using the *myo1A*^{ts}*-GAL4* driver) 0.5 or 120 hours after acute feeding with spores.

(E) Representative confocal images showing SA-11$^{R/G}$ spore germination in the anterior and posterior midgut of WT flies (Canton S) and *Rel*^{E20} mutant flies 6 hours after acute feeding with spores. DAPI (blue) marks the nuclei. Spores are in red, vegetative cells in green. The yellow fluorescence corresponds to germinating spores (see Figure 2A).

(F and **G)** RT-qPCR analyses of the expression of *AMPs* (F) and *amidases* (G) in *Rel*^{E20} mutant flies 4 hours after acute feeding with SA-11 spores. UC corresponds to flies fed with water.

Data represent mean ± SEM of at least four independent experiments. The Mann-Whitney test was used to analyze data in A-D. Student's t-tests were used to analyze data in F and G. *p≤0.05, **p≤ 0.01, ***p≤0.001, ns = non-significant.

Figure 6. Dif and Relish are synergistically involved in *Bt* persistence

(A and **E)** SA-11 bacterial load in midguts of *Dif*^{1} (A) or *Dif*^{1}*;Rel*^{E20} (E) homozygous mutants 0.5 or 120 hours after acute feeding with spores.

(B and **F)** Representative confocal images showing SA-11$^{R/G}$ spore germination in the anterior and posterior midgut of WT flies (Canton S) and *Dif*^{1} (B) or *Dif*^{1}*;Rel*^{E20} (F) homozygous mutant flies 6 hours after acute feeding with spores. DAPI (blue) marks the nuclei. Spores are in red, vegetative cells in green. The yellow fluorescence corresponds to germinating spores (see Figure 2A).

(C, D, G and **H)** RT-qPCR analyses of the expression of *AMPs* (C and G) and *amidases* (D and H) in *Dif*^{1} (C and D) or *Dif*^{1}*;Rel*^{E20} (G and H) homozygous mutant flies 4 hours after acute feeding with SA-11 spores. UC corresponds to flies fed with water.

Data represent mean ± SEM of at least four independent experiments. The Mann-Whitney test was used to analyze data in A and E. Student's t-tests were used to analyze data in C, D, G and H. *p≤0.05, **p≤ 0.01, ***p≤0.001, ns = non-significant.

Figure 7. *Bacillus* spore persistence leads to *amidase* expressions in the mouse gut.

(A) Schematic illustration of the procedure for oral gavage using SA-11 spores. Mice were kept in the same cage throughout the experiment. Small intestine samples were collected at t = 4, 24, 48, 120 and 240 hours after the gavage.

(B and **F)** SA-11 bacterial loads in split mouse small intestines after gavage using the mode of breeding shown in (A) for (B) and in (E) for (F). The vertical axis indicates the median number of CFUs per mouse.

(C and **G)** SA-11 bacterial load in different parts of the small intestines using the mode of breeding shown in (A) for (C) and in (E) for (G). Green bars (non-heated samples) represent the whole SA-11 bacterial load (spores and vegetative cells). Red bars (heated samples) represent the proportion of non-germinated spore loads. Data represent the mean ± SEM of at least five independent experiments.

(D) Monitoring of SA-11$^{R/G}$ spore germination in the small intestine 4h post-gavage. The lower panel represents plots of the average fluorescence intensity (the mean gray value) of

SA-11$^{R/G}$ measured along the small intestine in the upper panel. Red labeling corresponds to spores and green (GFP) corresponds to vegetative cells (GFP).

(E) Schematic illustration of the procedure for acute oral gavage using SA-11 *Bt* spore. Small intestines samples were collected at t = 4, 24, 48, 120 and 240 hours after the oral gavage. Breeding cage was changed initially 4 hours post-oral-gavage and then every day.

(H and **I)** RT-qPCR analyses of the expression of mouse amidases (*Pgylrp1* and *Pgyrlp2*) in different parts of the small intestine after spore ingestion using the mode of breeding shown in (A) for (H) and in (E) for (I). Error bars represent SEM (n=5). The student's t test was used to analyze statistical significance. *p≤0.05, **p≤ 0.01, ***p≤0.001, ns = non-significant.

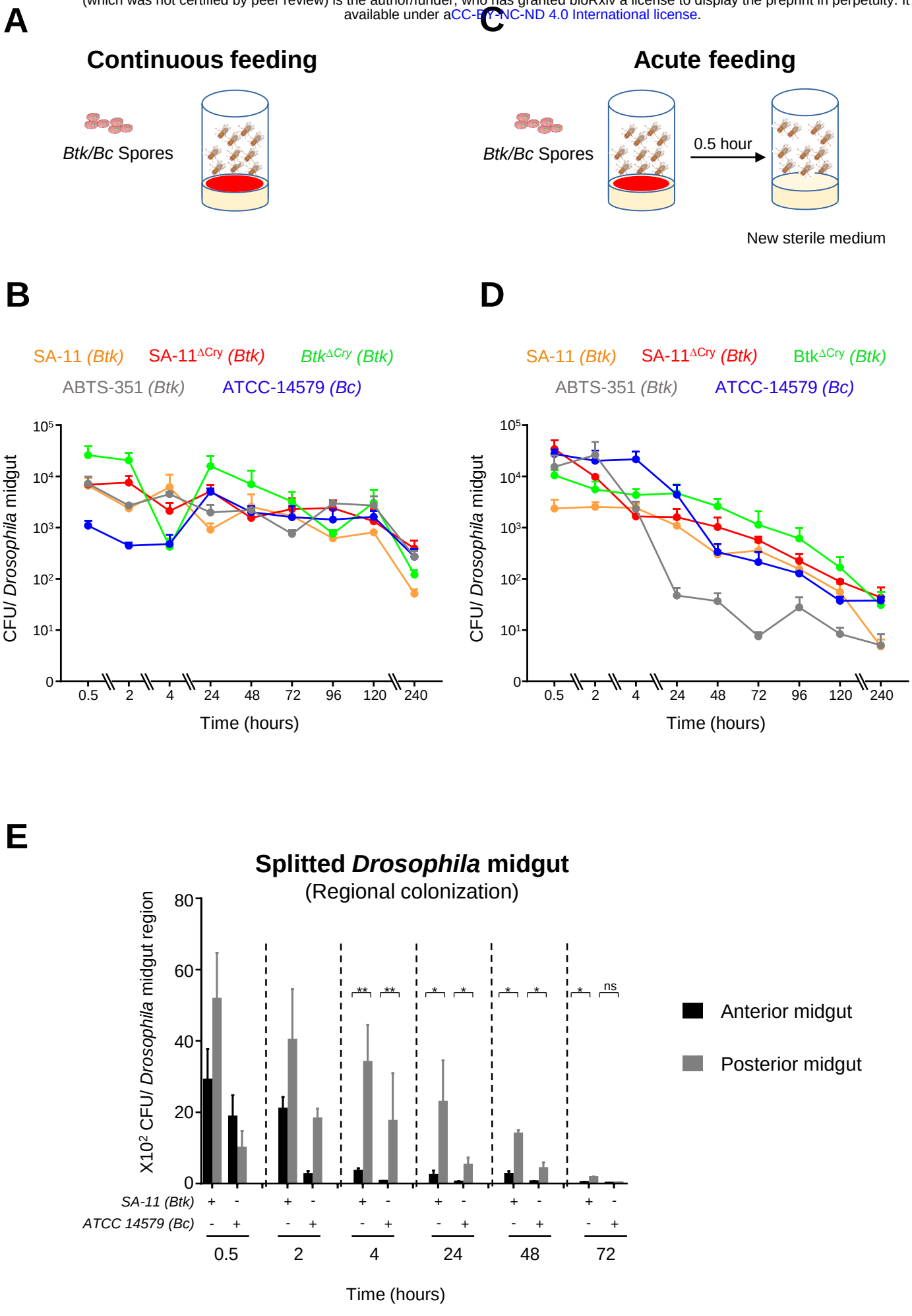

Figure1

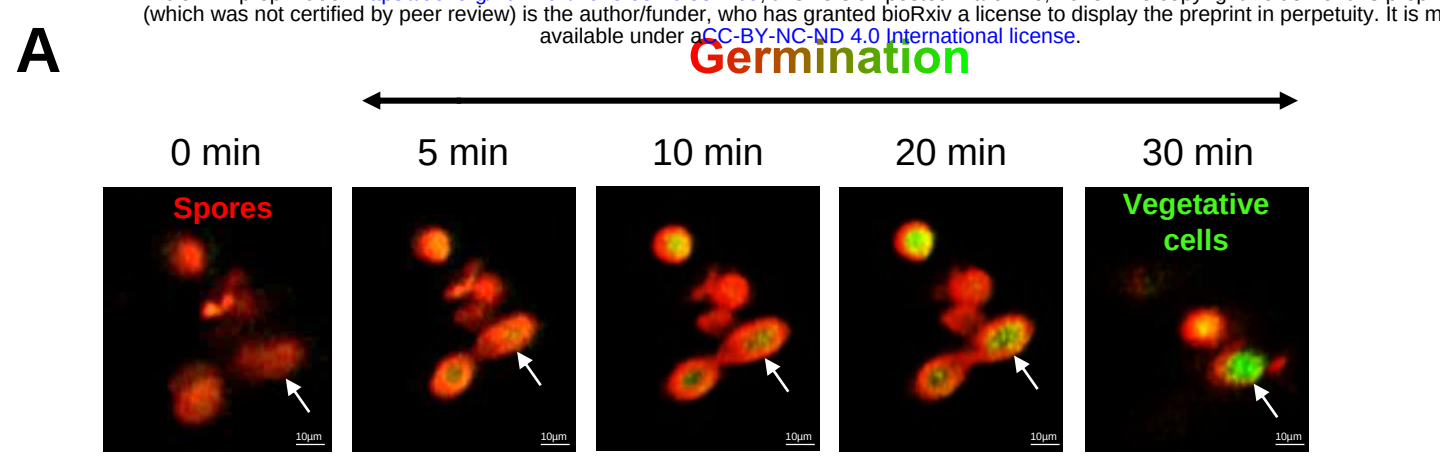

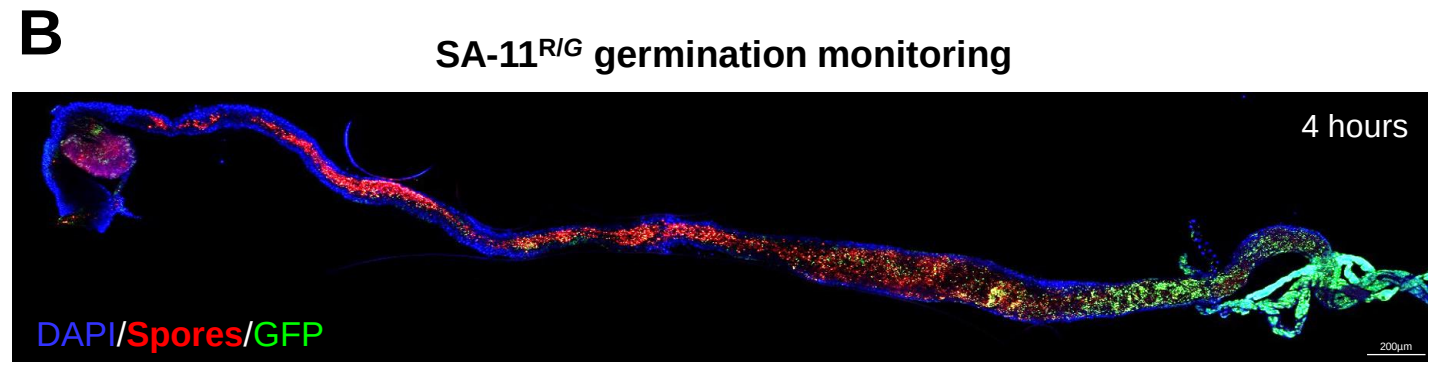

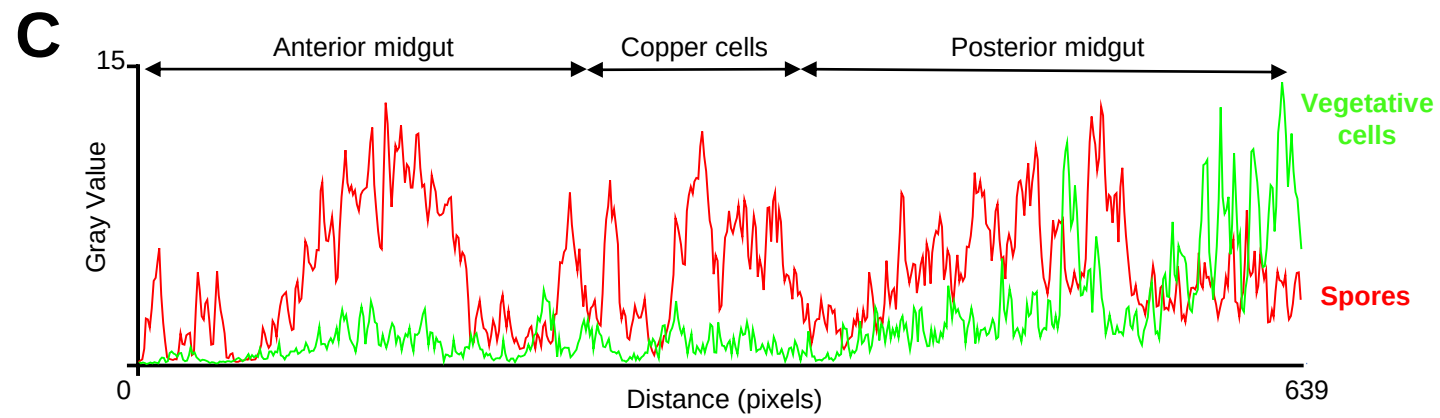

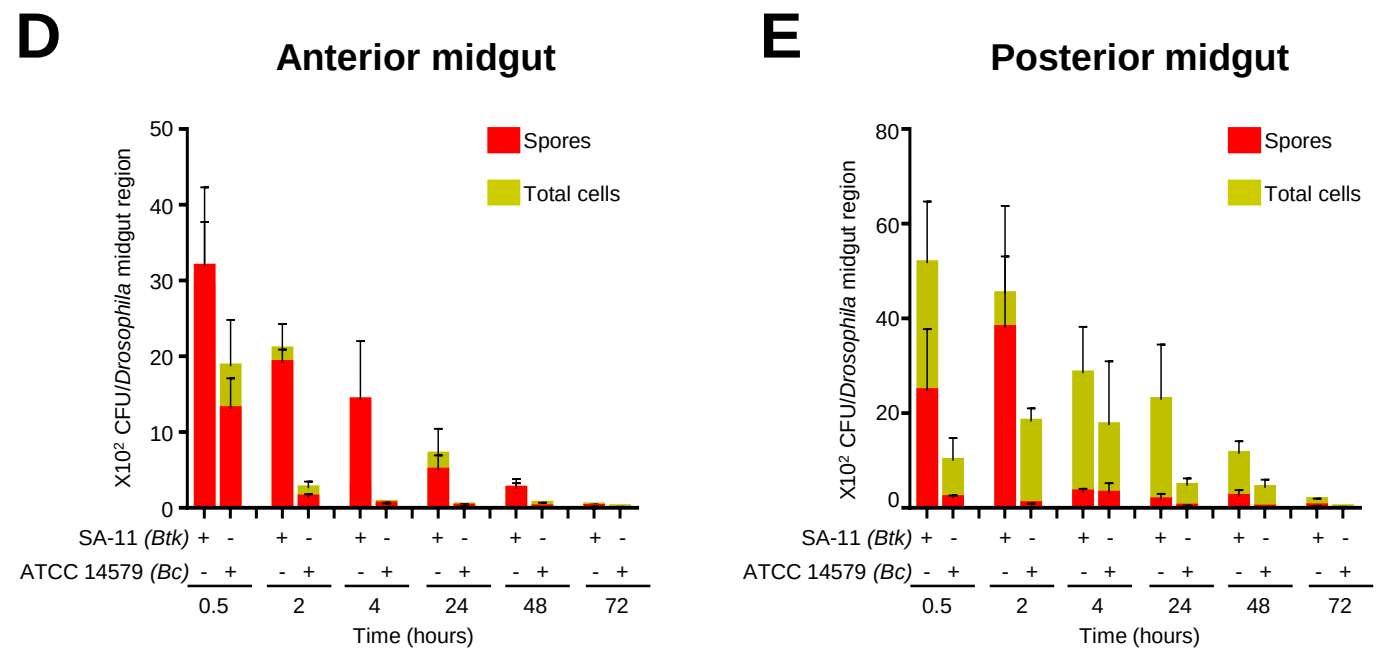

Figure 2

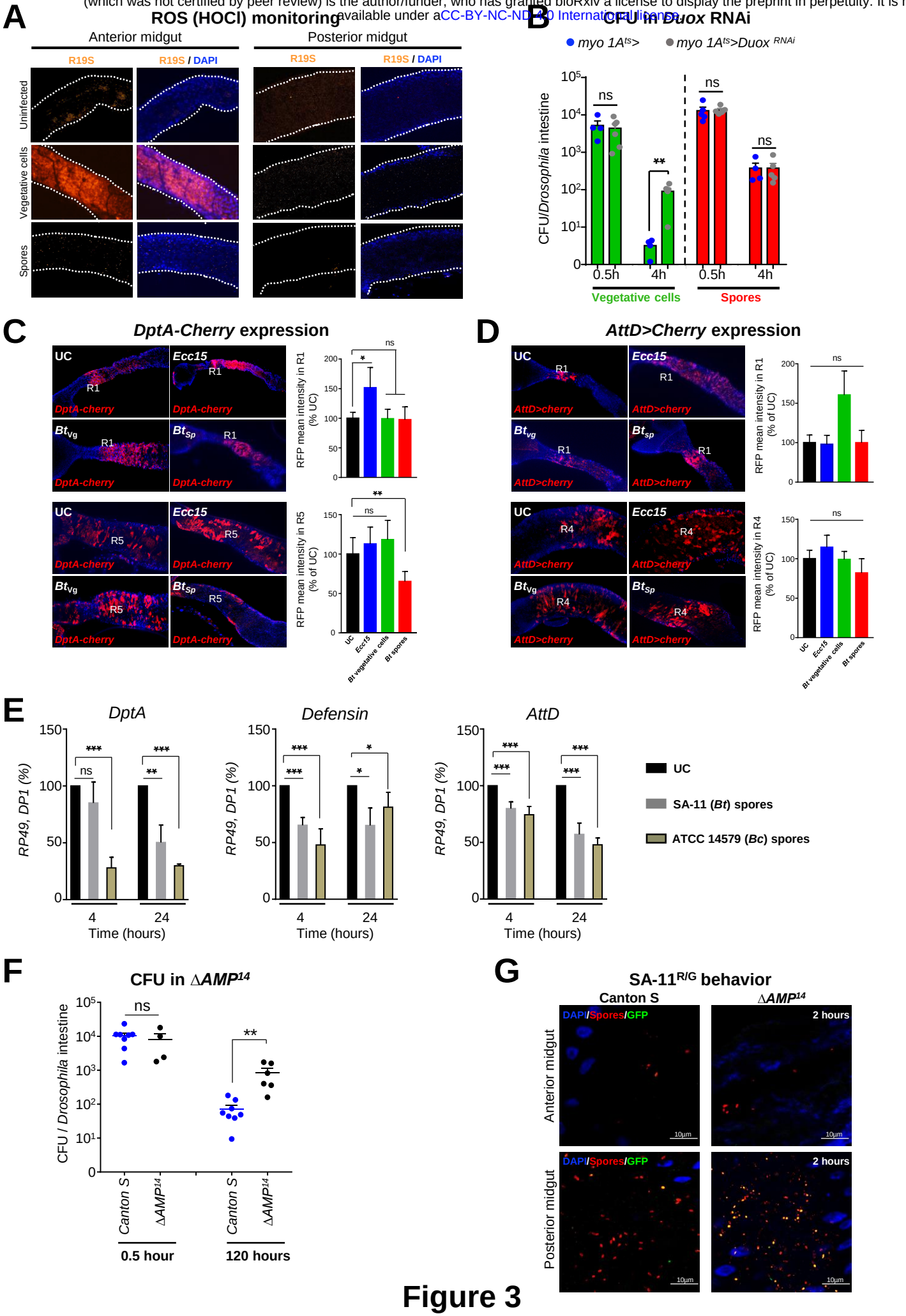

Figure 3

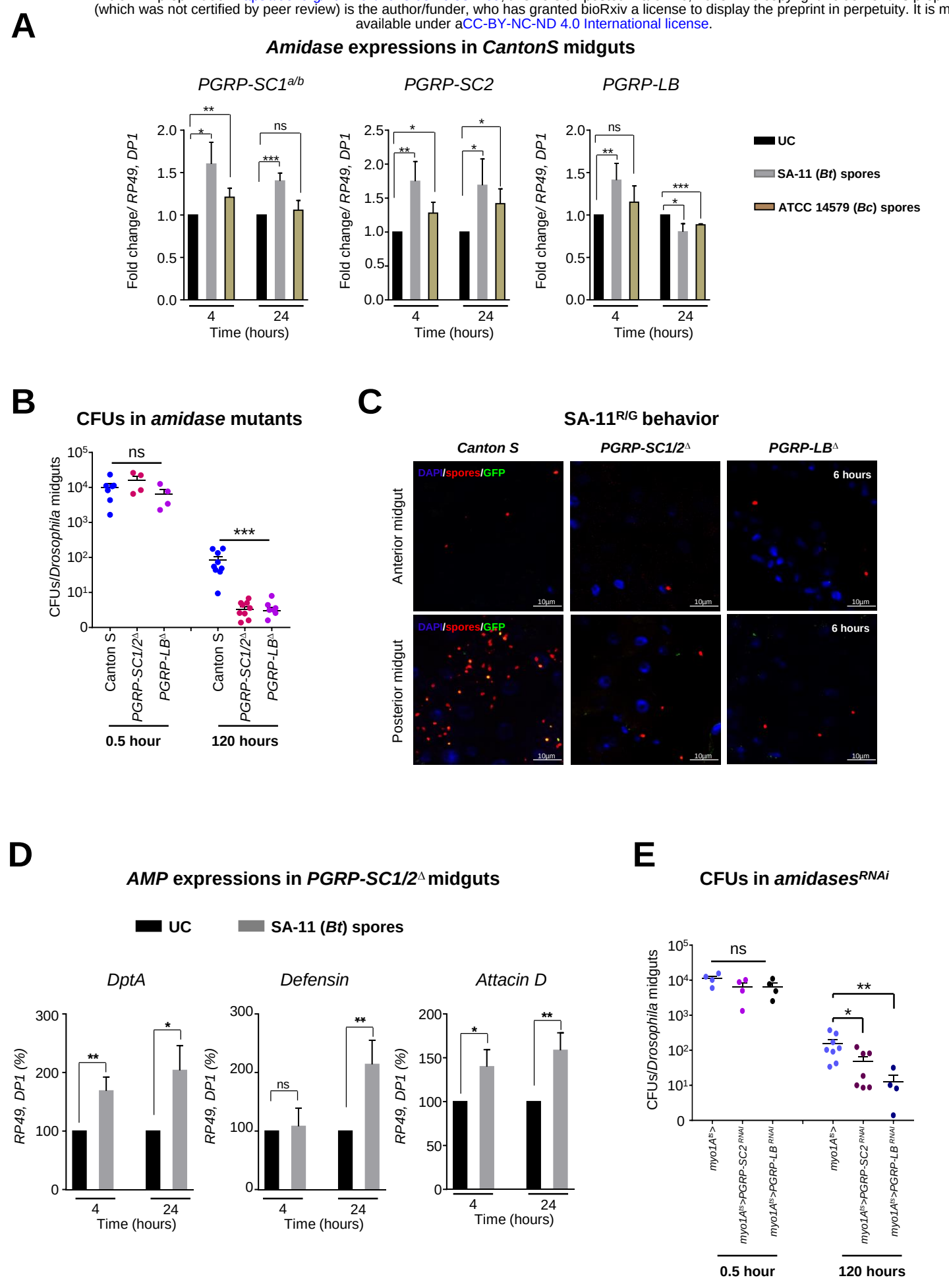

Figure 4

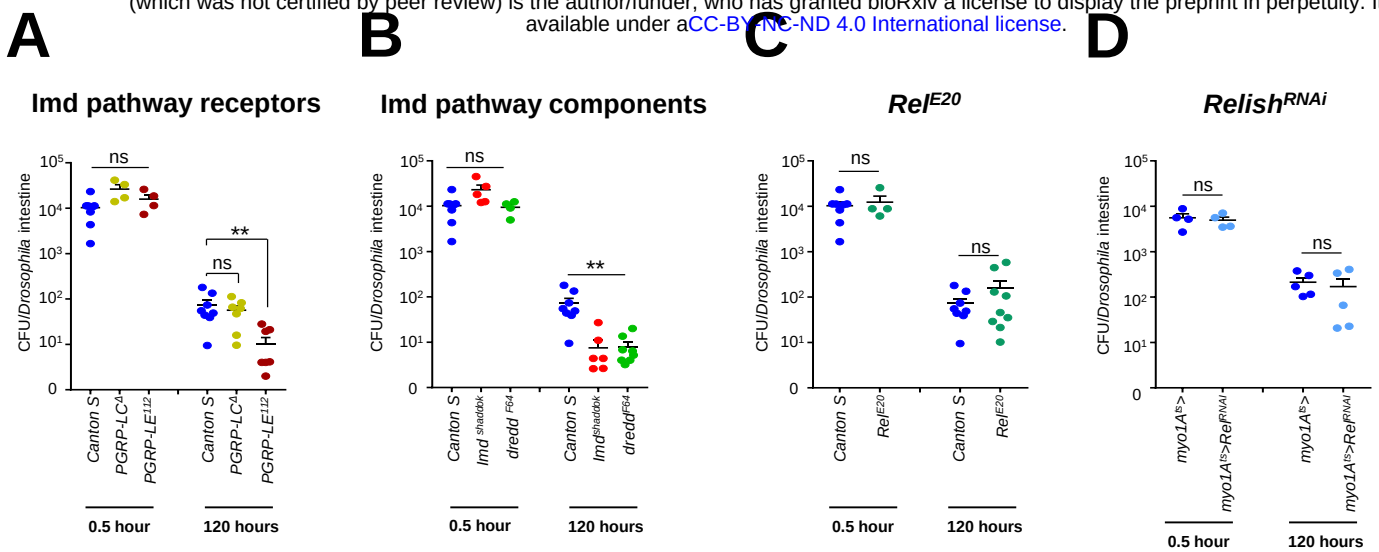

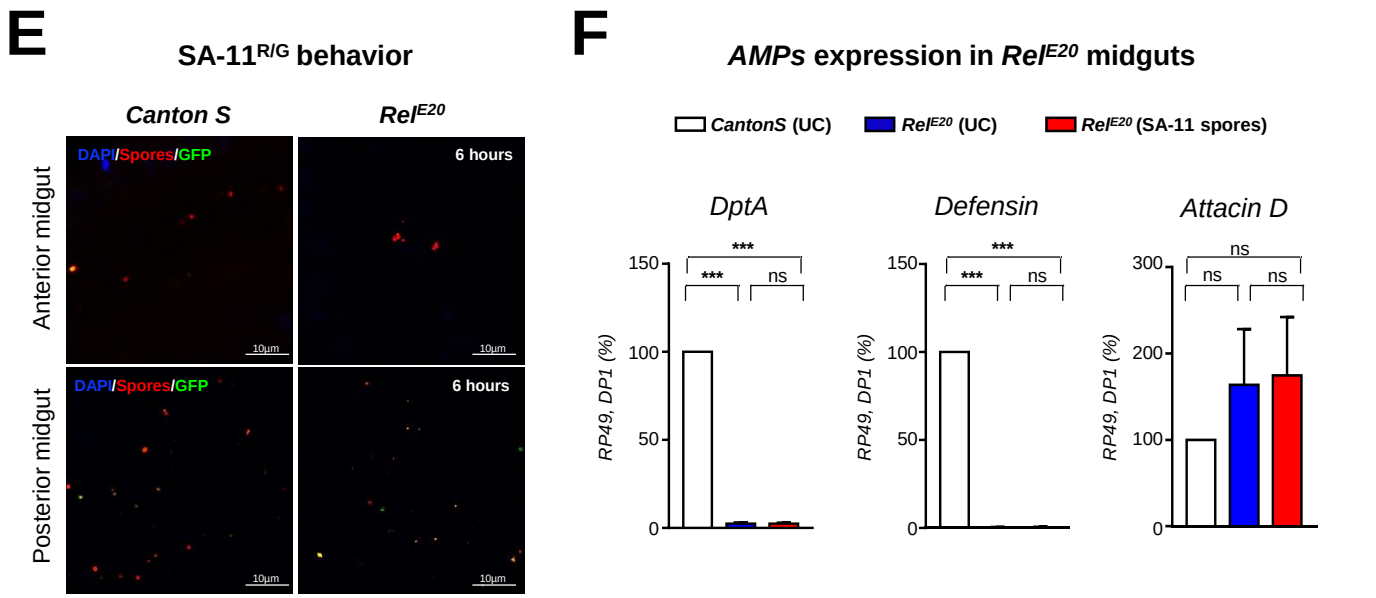

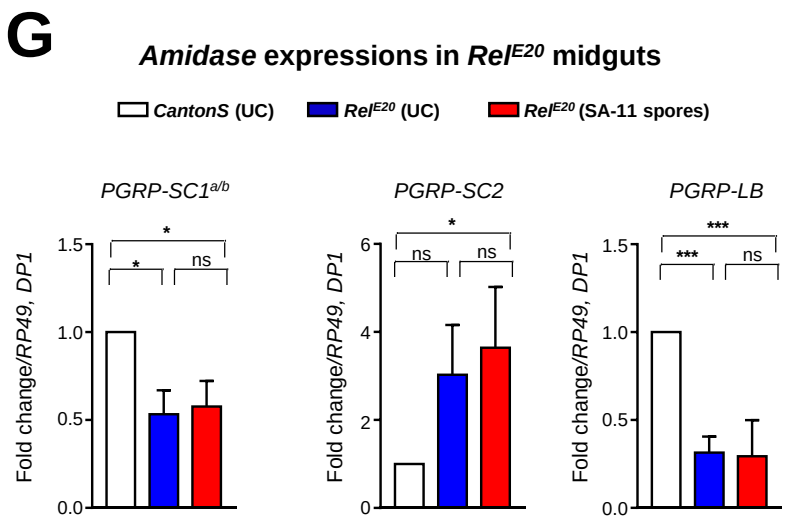

Figure 5

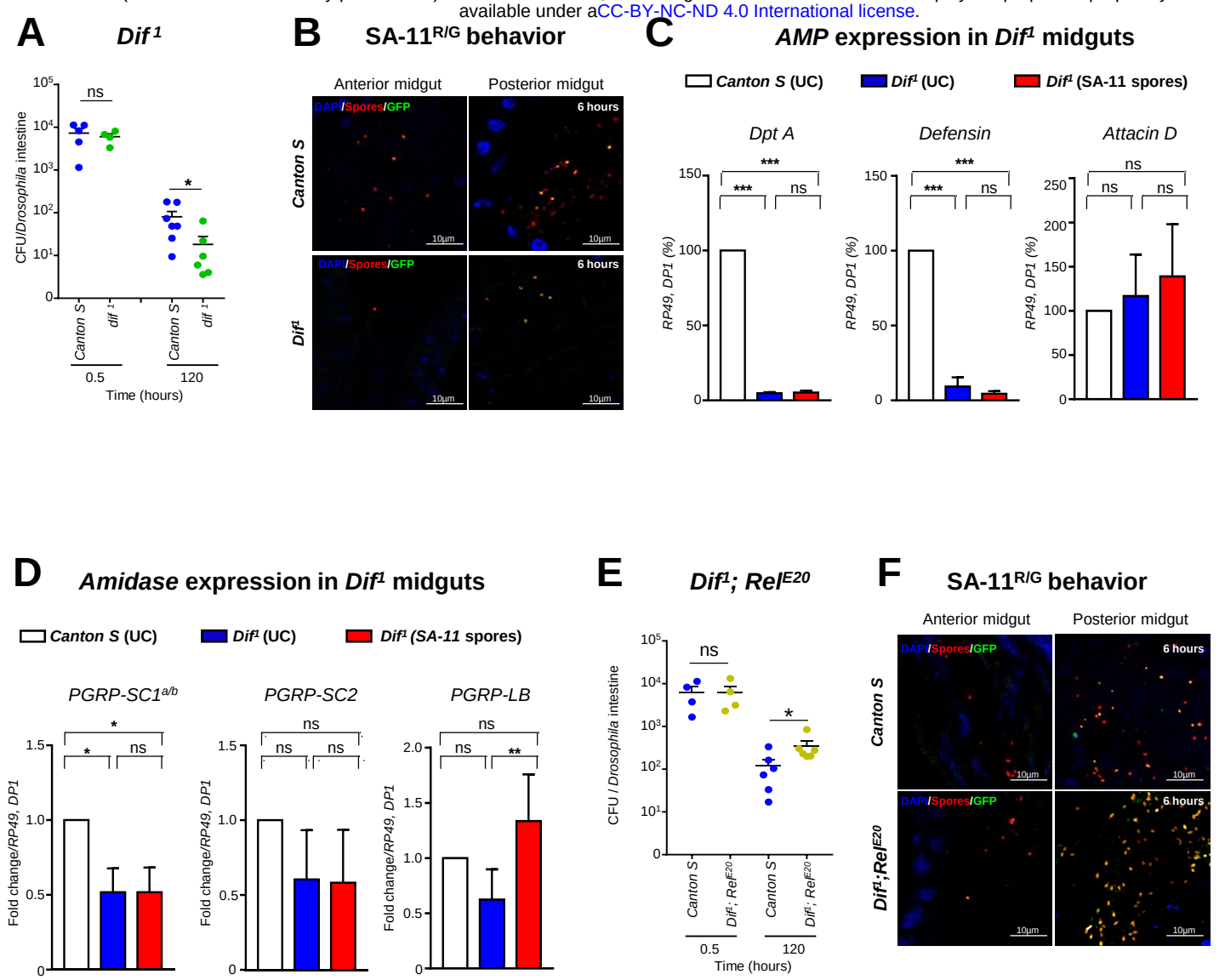

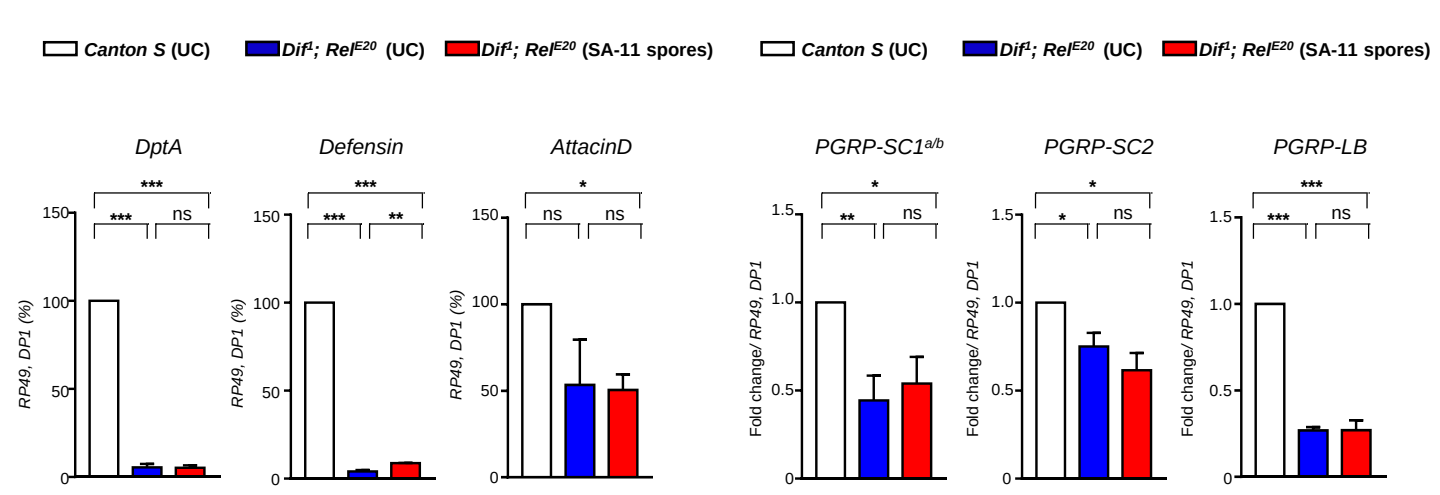

Figure 6

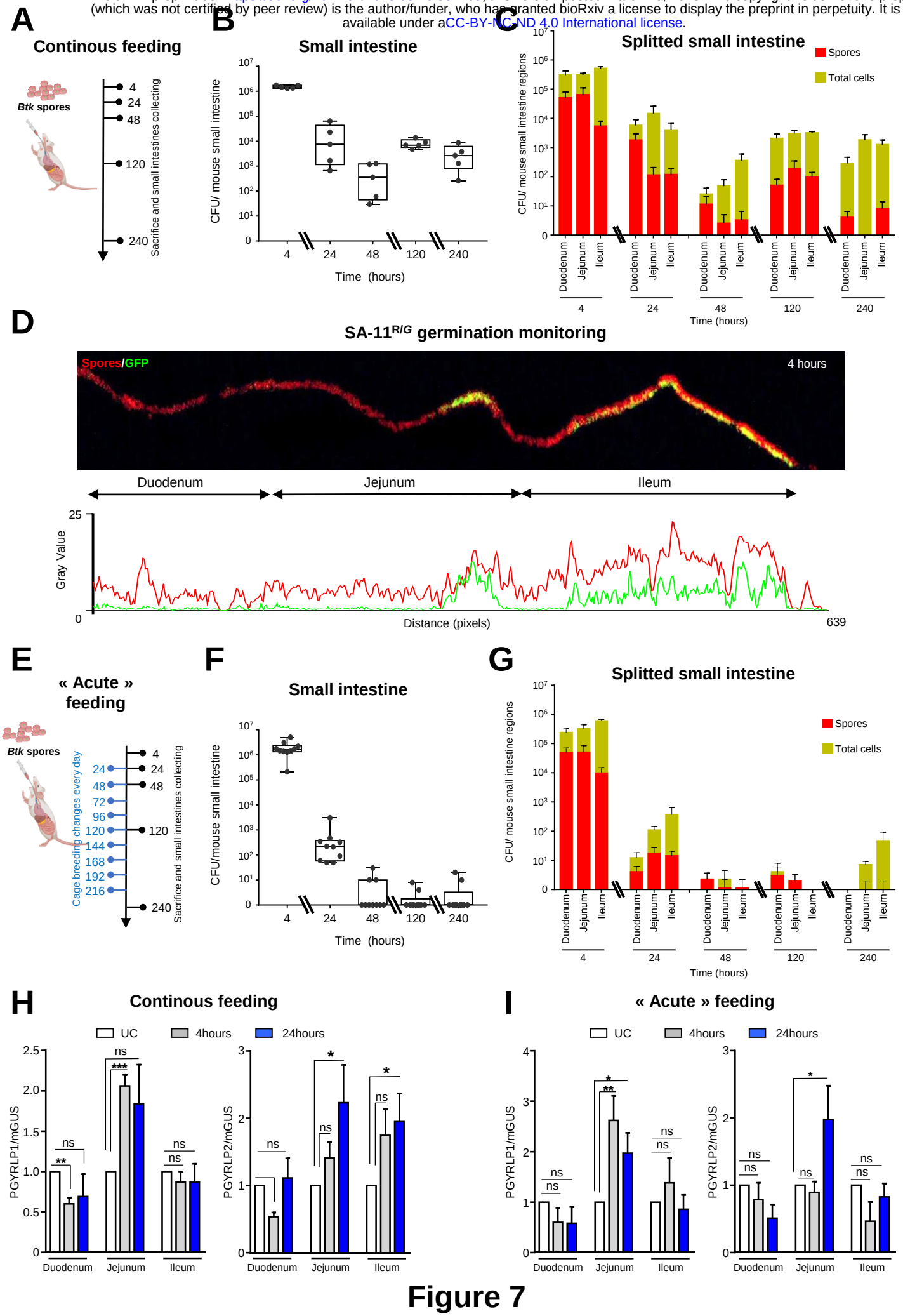

Figure 7